بسم الله الرحمن الرحيم

SUDAN UNIVERSITY OF SCIENCE AND

TECHNOLOGY

COLLEGE OF GRADUATE STUDIES

التحليل الآلي لأداء جهاز الجاما كاميرا باستخدام معالجة الصور

Automatic Analysis's of SPECT Gamma Camera performance using Image Processing

A thesis submitted for a Ph.D. degree in Medical Physics

BY

Einas Mohamed Ahmed

M.Sc in Medical Physics

Supervisor

Dr. Mohamed Elfadil

January 2014

بسم الله الرحمن الرحيم

قَالَ تَعَالَىٰ:

﴿ قَالُوا۟ سُبْحَٰنَكَ لَا عِلْمَ لَنَآ إِلَّا مَا عَلَّمْتَنَآ ۖ
إِنَّكَ أَنتَ ٱلْعَلِيمُ ٱلْحَكِيمُ ﴿٣٢﴾ ﴾

سورة البقرة الآية 32

صدق الله العظيم

Abstract

The main objective of this study was to assess the quality control of SPECT gamma camera using developed Algorithm via image processing procedure. Usually assessment done through visual inspection of phantom images i.e. visual perception trend; in this study separate algorithm were developed to quantify the uniformity (integral, and differential), linearity and resolution using Modulation Transfer Function (MTF). The data of this study were collected from Royal Care International Hospital, Nuclear Medicine Department in the period from 2014 to 2016; images of QC test were taken from SPECT gamma camera as DICOM format. The result of this study showed that the uniformity for useful central field of view for integral uniformity was 2.97%. While row differential uniformity was 1.96% and column differential uniformity was 1.55% similar to build in routine. The linearity showed that for vertical location the variation from the original location of the line it was 0.02 mm which indicates that almost the point's falls in the line with a correlation coefficient of 0.998. For horizontal lines the differences between the two in average equal to 0.2mm, with a correlation coefficient equal to 0.956. The resolution for minimum object used 4mm was 70% and increased with object size increased to reach 100% resolution for an object size of 10 mm i.e. 100% resolution corresponds to the coordinate of the MTF at 10% and frequency of 0.05cycle /mm. in conclusion the developed algorithm can be used to assess all gamma camera QC image regardless of the machine brand objectively.

المستخلص

الهدف الرئيسي من هذه الدراسة تقويم جودة القاما كاميرا سبيكت باستخدام خوارزمية مطورة عن طريق إجراء معالجة الصور. عادة ما يتم التقييم من خلال التفتيش البصري لصور المجسمات التحققية أي بأستخدام الإدراك البصري. في هذه الدراسة تم تطوير خوارزمية منفصلة لقياس الاستواء (التكاملي و التفاضلي)، والخطية والتباين باستخدام وظيفة تحويل التحويرية. تم جمع بيانات هذه الدراسة مستشفى رويال كير الدولي، قسم الطب النووي في الفترة من 2014 إلى 2016؛ صور اختبار الجودة أخذت من كاميرا غاما سبيكت في صيغة دايكوم. أظهرت نتائج هذه الدراسة أن استواء لمجال المركزي التكاملي كان 2.97٪. في حين كان الاستواء التفاضلي الصفي 1.96٪ والعمودي كان 1.55٪ اي مماثلة لروتين الجهاز. وأظهرت الخطية أنه بالنسبة للموقع الرأسي فإن الاختلاف عن الموقع الأصلي للخط كان 0.02 مم مما يشير إلى أن النقطة تقريبا تقع في السطر مع معامل ارتباط 0.998. أما بالنسبة للخطوط الأفقية، فإن الفروق بين المتوسطين يساوي 0.2 مم، مع معامل ارتباط يساوي 0.956. كان الحد الأدنى لللتباين للكائن المستخدم 4 مم 70٪ ويزداد مع زيادة حجم الكائن للوصول إلى 100٪ تباين لحجم كائن يساوي 10 ملم أي 100٪ تباين يتوافق مع وظيفة التحويل التحويريةعند 10٪ وتردد 0.05 دورة / مم. في الختام الخوارزمية المطورة يمكن استخدامها لتقييم جميع انواع القاما كاميرا بغض النظر عن نوع العلامة التجارية بموضوعية.

Dedication

To

MY FAMILY MOTHER FATHER BROTHERS AND SISTER

TO

MY FRIENDS

TO

EVERY ONE HELP ME

Acknowledgements

I am deeply thankful to ALLAH the beneficent, for the progress and success I

Gained in all my study It is a great pleasure to acknowledge all those people who had given me tremendous help and support in completing this study especially to my supervisor, Dr Mohmed Elfadil 'Sudan University of Science and Technology college of Medical Radiologic Science 'for his full guidance and assistance throughout the whole period of this study.

Special thanks to whole staff in Royal Care International Hospital in Khartoum, department of nuclear medicine

Also great thanks for everyone, who try to help, guide and encourage me to finish this work.

Finally, I am especially grateful to my family for their support through all my life stages.

Table of contents

List of Figures

Chapter one

Introduction

Nuclear medicine is critically dependent on the accurate, reproducible performance of clinical radionuclide counting and imaging instrumentation. Quality control (QC), which may be defined as an established set of ongoing measurements and analyses designed to ensure that the performance of a procedure or instrument is within a predefined acceptable range, is thus a critical component of routine nuclear medicine practice. An extensive series of parameters has been developed over the years for acceptance testing and performance characterization of γ-cameras, SPECT and PET scanners, and other nuclear medicine instrumentation. A quality control program is especially important in two main areas: instrumentation and radiopharmaceutical preparation (Zanzonico. P 2008)

1-1 Gamma Cameras

Scintillation camera systems are subject to a variety of detector and associated electronic problems that can cause aberrations of the image and may not be detected by the casual observer. Thus, quality control procedures are especially important to ensure high-quality, accurate diagnostic images. The three parameters usually tested are (1) spatial

resolution, or the ability to visualize an alternating, closely spaced pattern of activity; (2) image linearity and distortion, or the ability to reproduce a straight line; and (3) field uniformity, or the ability of the imaging system to produce a uniform image from the entire crystal surface. In general, these determinations can be made with or without the collimator.

(Fred A. M 2012)

To ensure high performance standards of single photon emission computed tomography (SPECT) cameras, routine detector quality control procedures should be performed weekly, as with any gamma camera, including tests of intrinsic uniformity, extrinsic uniformity (collimator in place), resolution, and linearity. Regular meticulous quality control of SPECT imaging systems is absolutely essential for the production of clinically useful, artifact-free images. Although even significant deviations from optimum performance can be tolerated in routine planar imaging .(Fred A. M 2012)

Documenting of QC procedures and organized recording of the results of such procedures are requirements of a sound, compliant QC program. A written description of all QC procedures, including the acceptable (or tolerance) range of the results of each such procedure and the corrective action for an out-of-tolerance result, should be included in the procedure manual of the facility; for each procedure, the written description should be signed and dated by the facility director, physicist, or other responsible

individual. For each QC test performed, the following data, as well as the initials or signature of the individual performing the test, should be recorded on a structured and suitably annotated form: the test performed; the date and time of the test; the make, model, and serial number of the device tested; the make, model, and serial number of any reference sources used; the results of the test; and a notation indicating if the test result was or was not acceptable (i.e., was or was not within the specified tolerance range). (Fred A. M 2012)

In many instances, QC tests of nuclear medicine instrumentation are performed not with the radionuclides that are used clinically but with longer-lived surrogate radionuclides in the form of so-called reference sources. Such standards are commercially available in various activities and geometries, depending on the application. (Gopal **.**B 2013)

Among routine dose-calibrator QC tests, constancy must be checked daily and accuracy and linearity at least quarterly daily checks of accuracy are recommended, however. At installation and after service of a dose calibrator, its geometry (position and volume)-dependent response for ^{99m}Tc must be measured and volume (from 2 to 25 mL)-dependent correction factors relative to the standard volume (e.g., 10 mL) derived.

For the constancy test, a reference source, such as ^{57}Co, ^{133}Ba, ^{68}Ge, or ^{137}Cs, is placed in the dose calibrator, and the activity reading on each

scale is recorded; day-to-day readings should agree within 10%. For the accuracy test (also sometimes known as the energy linearity test) (Gopal .B 2013)

The routine QC tests for well counters include checks of the photopeak energy window (i.e., energy peaking) if the counter is equipped with an MCA and of background, constancy, and efficiency (or sensitivity). Before counting samples containing a particular radionuclide, one should check the energy spectrum to verify that the counter is properly peaked, that is, that the photopeak of the radio-nuclide coincides with the preset photopeak energy window. Isotope-specific radionuclide counting or imaging with a scintillation detector commonly is done using a 20% photopeak energy window, equivalent to an energy range of $E_\gamma \pm 10\%$ (i.e., 0.9–1.1 E_γ), where E_γ is the x- or γ-ray energy of the radionuclide.

The principle of tomographic imaging in nuclear medicine is based on the detection of radiations from the patient at different angles around the patient. It is called emission computed tomography (ECT), which is based on mathematical algorithms, and provides images at distinct depths (slices) of the object ,In contrast, in transmission tomography, a radiation source (x-rays or a radioactive source) projects an intense beam of radiation photons through the patient's body, and the transmitted beam is detected by the detector and further processed for image formation.

The most common SPECT system consists of a typical gamma camera with one to three NaI(Tl) detector heads mounted on a gantry, an online computer for acquisition and processing of data, and a display system(Gopal .B 2013)

1-2 Problem of the study:

The evolution of the Quality images of planner and SPECT gamma camera Depend on visual perception which is a subjective evolution, therefore if the images scored objectively using prototype algorithm a quantitative and objective method will be sustained.

1-3 Objective

The general objective of the study is to used an automatic method to analyze quality control test images of SPECT gamma camera using image processing in order to have an objective scoring

Specific objective:

- To develop an algorithm that read and analyses the Gamma camera quality control images.

- To measure the spatial resolution of gamma camera images using modulation transfer function.
- To measure the uniformly(integral and differential)

1-4 Significance of the study

This study will provide and automatic and quantitative method to evaluate the gamma camera performance through an objective method

1-5 Overview of the study

This study is concerned with assessment of gamma camera QC images using developed algorithm accordingly, it falls into five chapters. Chapter one is an introduction, which include introductory notes on gamma camera and quality control, as well as statement of the problem and study objectives. While Chapter two included a comprehensive scholarly literature reviews concerning the previous studies. Chapter three deals with the methodology, where it provides an outline of material and methods used to acquire the data in this study as well as the method of analysis approach. While the results were presented in chapter four, and finally Chapter five include discussion of results, conclusion and recommendation followed by references and appendices.

Chapter two

Literature review

Vickery et.al (2011) developed software program for gamma camera quality control based on NEMA NU-1 2007, Within Nuclear Medicine, image abnormalities and artifacts affecting the quality of images are well known phenomena. Therefore, it is of great importance to have a thorough Quality Assurance for gamma and SPECT cameras to minimize the occurrence of these abnormalities and artifacts. NEMA has made recommendations of routine quality control for nuclear medicine instrumentation. After installation and before the camera is put into clinical use, it should undergo National Electrical Manufacturers Association (NEMA) Performance standard measurements to verify that the camera performs according to specification supplied by the manufacturer and to establish baseline conditions for all future measurements. The NEMA Standards Publication NU 1-2007 describes how to perform process and report QC tests for gamma and SPECT cameras. Often, with support from the manufacturers, all necessary phantoms can be supplied and acquisitions can be done according to NEMA, but a thorough Quality Assurance also requires a careful handling of the measured QC data. The software is based on NEMA

recommendations regarding processing and analysis of the data, and runs in MATLAB (Math works, Natick, Massachusetts, USA). It is capable of calculating Intrinsic Spatial Resolution and Linearity (ISR & ISL), Intrinsic Energy Resolution (IER), Intrinsic Flood Field Uniformity (IFFU), Multiple Window Spatial Resolution (MWSR), Intrinsic Count Rate Performance (ICRP), System Spatial/Scan Resolution (SSPR & SSCR), System Planar Sensitivity (SPS), System Alignment (SA), System Volume Sensitivity (SVS) and SPECT Reconstructed Spatial Resolution (SRSR). The data handling programs are aimed at making the processing of acquired QC-data a simple task, providing the users with instructive images of the processed data as well as text files containing the results of the QC. Results processed with different software and for different SPECT the researchers demonstrated that whom software is able to calculate several NEMA-specifications, and where possible, the results were compared to those obtained by the manufacturers. And there is an agreement between our software and the manufacturers' software. A novel quantitative analysis of orthogonal hole and quadrant phantoms was presented. The selection of the platform used to code the software was MATLAB, which, in principal, is independent of the operating system. Future development could be the compilation of our software, making it independent of the MATLAB environment and an automatic

report-generation using e.g. LaTeX. It is whom vision that the software will be open access.

Ng et al. (2008) developed a simple sphere phantom for routine performance test of Single Photon Emission Computed Tomography (SPECT) gamma camera to be use in situation where the commercial expensive phantom is not available. The design of the low cost phantom was based on the common parameters measured using commercial phantom; these parameters are spatial resolution, contrast and sensitivity. The design of house phantom was based on the design of Perkins et.al. (2007). The phantom was consist of combination between the abdomen Computed Tomography (CT) phantom and acrylic support and based constructed in an (L) shape originally designed with circular array of blind hubs to hold laver lock syringes in a perpendicular array. The angle between each holder was 60^{o} and the diameter across two opposite holder was 100mm. when filled with radioactivity the syringe would form standard source of radioactivity in a reproducible configuration, so that they seen as parallel rods during image reconstruction. All imaging of phantom was carried out at university of Malaya using a triple detector SPECT camera (Philips IRIX, USA). The scanning time and injected activity of the performance test evaluation recommended by NEMA-1

(2001). The sphere was filled with a range of concentration of ^{99m}Tc between 58 and 101MBqmL^{-1}. The phantom was placed on the couch and SPECT acquisition was performed using 120 continuous scanning mode with incremental views of 3^{o} each time of acquisition with 90 min and the images were reconstructed on an Odyssey lx computer using filter back projection for 128X128 matrix size. In comparison, the cost of new phantom was 703 dollar while the commercial one was 2050 dollar. The first and obvious difference between the phantoms was that the sphere test was designed to measure hot spot detection, whereas the Jaszczak phantom demonstrated cold spot detection. The Jaszczak phantom required a nominal 750MBq or higher activity for use, while the sphere phantom could be used with less than 50% of that activity (of the order of 370 MBq). Increasing sphere volumes from 0.55 to 2.60 mL resulted in increase in contract. However a saturation effect was observed for higher volume. They lack from numerical result of the essential SPECT test, so the comparison of result to that of Jaszczak phantom was shorted. This phantom has advantage to do spatial resolution, linearity, uniformity, hot and cold contract, lesion detect ability and object size while the phantom cannot measure the Center of rotation (COR).

Alain (2010) performed and assessed all primary and some secondary NEMA-NU1-2001 performance test on two Brightview Philips cameras

and two hybrid camera with computed tomography (CT) named Brightview XCT Philips system installed 2009 in institute of physics Belgium. The materials used was four Philips camera fitted with a 9.5mm thick NaI crystal, 9.28mm pixel size with 64X64 matrix size and the activity used was measured using Veenstra VDC-405 activity meter. The primary NEMA tests as well as intrinsic linearity and system sensitivity was performed using ^{99m}Tc with LEHR collimator fitted. Multiple window spatial registration was performed with ^{67}Ga on one SPECT-CT camera. The Philips jet stream reconstruction tools were used for SPECT reconstruction with filtered back projection reconstruction and a ramp filter without cutoff used. The data processed according to NEMA NU!-2001 using the NEMA package of the Philips Pegasus (Brightview) or EBW (Brightview XCT) software. The result showed that the Multiple window spatial registration was 0.55+/- 1.5 with ^{67}Ga, the measured sensitivity were 73.5 +/- 1.5 cps/MBq for LEHR collimator and ^{99m}Tc, and 94.1 +/- 2.6 cps/MBq for medium energy collimator and 67Ga, and 47.0 +/- 1.3 cps/MBq for high energy collimator and 131I. The relationship between input and output count rate was found to be strictly linear up to a minimum of 30 Kcps for all heads. The maximum count rate was 239.8 +/- 3.3 Kcps and the observed count rate at 20% loss was 238.8 +/- 4.0 Kcps. The mean average distance between the SPECT and CT images was 1.34 +/- 0.57 mm and the maximum differences distance

was 1.93 +/- 0.58 mm. Spatial resolution in UFOV is 3.17mm, resolution in CFOV FWHM 3.12mm, Spatial linearity in UFOV is 0.27, Spatial linearity in CFOV is 0.20mm Differential . The most important feature of this study was probably the opportunity to perform the NEMA tests on four SPECT cameras located in the same nuclear medicine department. Indeed, most of the NEMA data available in the literature were obtained on one single system. The measured parameters were almost identical for all the tested systems, and the vast majority of measurements were within manufacturer's specifications. The only exceptions were some of the uniformity indexes of two of the heads, but a new calibration solved the problem. The results obtained for the hybrid and stand-alone systems were very similar.

Andrew et al. (2007) developed software programme for gamma camera quality control based on National Manufacture Electric Associations (NEMA). The programme language selected by the researchers was MATLAB because it offers programming simplicity and offer excellent image processing and plotting capacities and features built –in digital image and communication (DICOM support. Another attractive feature of MATLAB is the graphical users interface (GUI) design environment. This drag-and-drop user interface design tool allowed quick prototyping of the application user's interface. Also the main advantage of MATLAB

is the user can get MATLAB copy to execute or programme without complicating license requirement. By installing the free MATLAB common runtime (MCR) any one can run our software, even if they do not Owen a license for MATLAB or the image processing toolbox. MATLAB is used and accepted in both industry and academia to a degree which gives the researchers confidence that, despite being a private company offering. MATLAB is a safe choice in term of both longevity and cross-platform support. The nuclear medicine quality control software (NMQC) designed by researchers can read image and header information from DICOM files, which have become a generally recognized format for medical imaging file and also support interfile format which is still used in older nuclear medicine camera. The basic design principle of NMQC was to closely follow (NEMA) recommendation regarding processing and analysis of the data. The NMQC software has ability to measure uniformity, profile analysis, center of rotation evaluation, tomographic uniformity measurement, planer uniformity trend analysis and other wide range of gamma camera quality control tests. NMQC software runs on Microsoft Windows, Linux, Apple's Mac Os X, and Sun Solaris. NMQC software has been tested on numerous gamma camera models, including GE Infinia and Infinia Hawkeys, Soph-GE DST; Philips Forte, Skylight and Vertex; and Siemens Ecam, MS2, MS3, DIACAM, orbiter and Symbia Cameras.

Connor et al. (2000) discussed the parameters used to evaluate the gamma camera quality control and the factor that affect the result of this parameter. There are a large number of factors that contribute to the final image quality including uniformity, resolution (intrinsic and energy), collimation and the hard copy device. The most sensitive parameter to change in system performance is system uniformity. The change in photopeak location, photo multiplayer tube performance, energy and linearity correction all affect the image uniformity. Uniformity measurement can be performed intrinsically using a small (□100μCi) ^{99m}Tc point source placed at a distance of four time the detectors Field of View (FOV), or can be measured extrinsically using either a solid disk of ^{57}Co or plastic phantom source containing ^{99m}Tc mixture in water. The disadvantage of intrinsic measurement is the remove of collimator which may result in crystal fracture, while the disadvantage of extrinsic measurement is the time taken in preparing the source and the consequential radiation exposure to the technologist. All of these problems can be avoided by careful preparation of the sheet source and by routine inspection of the source to check for warping, leakage or distortion of plastic. Measurement of system resolution and/or linearity

was generally performed on a weekly basis and can be performed using either intrinsic or extrinsic technique. To evaluate the spatial resolution of the gamma camera, a wide Varity of test patterns have been developed over the years. The most common test pattern is the four quadrate bar phantom, which account for over 80% of all resolution patterns used in nuclear medicine. The BRH and Hine Duley phantom can also be used to measure spatial resolution. Under most circumstances, intrinsic measurement is preferable to extrinsic measurement even the intrinsic one have disadvantage of attendant risk to the crystal. As to researcher experience the parameter of spatial resolution and linearity tend to be a very stable parameter and will often remained unchanged even in the presence of significant changes in image uniformity. The 4-quadrant bar phantom is the most commonly used phantom for measurement of system resolution, it is not ideally suited to the assessment of system linearity. Hence, test patterns such as the orthogonal hole pattern or the parallel line equal spacing phantom are preferable to the four-quadrant phantom as they allow assessment of both linearity and resolution. The international atomic (IAEA) and the national electrical manufacturing association (NEMA) presented details discussed to this parameter at year 2001 (NEMA-2001 and IAEA-TECDOC-602) while this work was presented at the year 2000, but there was no significant differences between the

methods of uniformity, linearity and resolution before and after the year 2001

Minarik et al. (2008) designed phantom to implement simulation of bremsstrahlung imaging in the SIMIND code and to validate simulations against experimental measurements, to investigate the image quality of clinical bremsstrahlung Single Photon Emission Computed Tomography(SPECT) imaging and to evaluate the quantitative accuracy for liver and tumor-shaped sources, using phantom studies Also to investigate the improvement obtained by applying model-based attenuation, scatter and collimator–detector response compensations in the reconstruction of SPECT image. ^{90}Y is rare-earth metal emit beta with mean energy of 0.935Mev and used in treatment of some malignant disease especially non-Hodgkin's lymphoma. Lack of gamma ray is a disadvantage in calculation of pre-therapy dose. ^{111}In is chemically similar to ^{90}Y but two problem associated with ^{111}In when use as pre-therapy dose calculation and post-therapy evaluation, the first problem is that free ^{111}In have different biokienetic of free ^{90}Y , the second problem is that the contribution to the image from bremsstrahlung generated by the β-particles emitted by 90Y probably affects the measurement of 111In. If the quantitative accuracy of the bremsstrahlung imaging is sufficiently accurate, it will also be possible to investigate the consistency

of the Dosimetry estimates between 111In-based pre-therapy and 90Y-based therapy studies. To perform patient-specific Dosimetry, one needs to apply quantitative methods to correct for scatter, photon attenuation and the degradation in spatial resolution due to the design of the collimator. This can, to some extent, be made in planar scintillation camera imaging using the conjugate-view method, but generally SPECT is preferred. Several problems associated with use of ^{90}Y bremsstrahlung imaging for quantitative imaging especially when using SPECT camera which are, very complexes energy spectrum and, photon scattered from patient. Bremsstrahlung spectra for water, soft tissue and bone were generated with the MCNPX Monte Carlo program by simulating a 90Y point source located in the center of a sphere, the amount of created bremsstrahlung photons was determined as a function of energy as they passed the surface of the sphere. Also a measurement was performed with a high-purity germanium detector (HPGe). To evaluate the ability of the SIMIND program to simulate accurate bremsstrahlung images, a comparison between measurements and corresponding simulations was performed using a 1 mL plastic syringe as a small cylindrical source, the syringe had an inner diameter of 4 mm, an outer diameter of 6.5 mm and a length of 65 mm, and was filled with a solution of 90Y up to a length of 60 mm, three measurements were performed with source-to-collimator distances of 10 cm, 20 cm and 30 cm, respectively. The camera system

was a hybrid SPECT/CT Discovery VH system (General Electric Medical Systems, Milwaukee, USA) with a 25.4 mm thick NaI (Tl) crystal, the measurement was made with a high-energy general-purpose (HEGP) collimator and a 60% energy window centered at 150 keV. Also the researchers used the RSD thorax phantom (Radiological Support Services Inc., Long Beach, CA) with activity uniformly distributed in the liver insert , measurements were conducted without background activity, and with a liver-to-background activity ratio of 10:1 , measurements were also performed using an elliptical water phantom (Data Spectrum Inc., Hillsborough, NC) with activity filled in a sphere with an inner diameter of 60 mm without background activity, the same collimator and energy window settings that were used for the syringe measurement were applied. Also the camera sensitivity was measured using Petri dish containing a thin layer of 90Y with an activity of 104 MBq. Also images of real patient were performed to the patient already treated with 90Y using SPECT/CT camera. All images were reconstructed using program developed by Frey et al. The result of this study showed that the percentage number of emitted bremsstrahlung photon per decay was 2.20. 2.23 and 4.39% for energies from 50Kev to maximum electron energy. The Full width at Half Maximum (FWHM) was 13.8, 18.3 and 23.8mm for 10, 20 and 30 cm respectively, and the Full Width at Ten Maximum (FWTM) was 26.6, 33.7 and 42.5mm for 10, 20 and 30 cm respectively.

Porras et al. (2002) developed and clinically tested a small, portable, and low cost gamma camera for medical application. The mini gamma camera has an overall size of 95mm in diameter and 240mm length, and total weight of 3 Kg. both, small dimension and light weight ensure the mobility of the system, which was one of the key pints of researcher design. The camera was optimizing for ^{99m}Tc emitting at 140KeV. The camera composed of a collimator, a circular scintillator crystal coupled to a position sensitive photomultiplier tube (PSPMTs). The collimator has hexagonal parallel holes lead (1.2mm diameter holes, 0.2mm of septal thickness and 35mm long) providing about 120 cpm/µCi of nominal geometric efficiency. The scintillation crystal used has dimension of 51mm made from CsI (Na) with white painted entrance pace and black edge. Geant-3 and Detect 2000 package was used. The photomultiplier tube used was Hamamatsu R2486 PSPMT that enables the acquisition of 2-diminsional information providing 4 signals (2X + 2Y) and has an effective area of 50 mm diameter. Physical measurements according to the National Electrical Manufacture Association (NEMA) have been performed in order to evaluate the camera performance. The researchers adapt the NEMA protocol to be useful for the mini gamma camera because NEMA protocol developed to be using in large system. The sources used include a 2mm diameter point source, 2mm capillary tube

source and a 6cm diameter plastic Petri dish for a uniform flood source. The intrinsic spatial resolution was measured as Full Width at Half Maximum (FWHM) for Useful Field Of View (UFOV) (2.2mm) and Central Field Of View (CFOV) (1.6mm) while the extrinsic spatial resolution measured with scatter (4.2mm) and without scatter (3.2mm). The differential linearity is 0.2 and 0.1mm, absolute linearity is 1.3 and 1.1, intrinsic absolute uniformity 93.6% and 41.3% and the extrinsic absolute activity are 73.1% and 49.9% for both UFOV and CFOV respectively. The system energy resolution is 12.8% at 140KeV. The system planer sensitivity is 104.7cpm/µCi. System dead time is 26.6µs. the result showed that there was no variations depending on the slit orientation but, as researcher expected, best values are obtained at the CFOV. The researcher used MLPE as reconstruction methods because it work well when using parallel hole collimator and, furthermore, allows reconstruction on real-time. A clinical test was performed on a thyroid phantom using ^{99m}Tc with a total activity of 200µCi, showed that the system produced high quality images of a real thyroid with the usual dose (2mCi) in an about 10min.

Elshemey et al (2013) evaluated the effect of scatter radiation on the performance of the gamma camera specially the extrinsic sensitivity and counting efficiency using a specially designed home-made phantom. An

acrylic cylindrical phantom was constructed, providing a cylindrical distribution of ^{99m}Tc, made from Perspex and glass with diameter of 0.32mm, a height of 0.25mm and thickness of 25mm. the gamma camera used was Symbia SPECT/CT, Siemens, Germany with low energy parallel hole general purpose collimator and 59 photo multi player tubes, the thickness of the crystal was 9.9mm. The phantom was filled with water up to 12mm, and then ^{99m}Tc was injected with activity of 0.2=+/- 0.01GBq. the energy spectrum was then acquired at different source level 50, 100, 150 and 200 mm. only one head (facing the ceiling) of the dual head camera was used in the acquisition of the energy spectrum. The scattered fraction was calculated from the energy spectrum. The shape of the photopeak at 140KeV does not noticeably change with source thickness, but there was a gradual increase in the scattered photon energy (133-153 Kev) due to the increase in probability of multiple scattering of photon inside thicker source. The scatter fraction increased with increasing source thickness, from0.29 up to 22.96. a decrease in the calculated extrinsic sensitivity, from 121.36 to 49.58 counts/s GBq at SDD ¼ 0.7 m with uncertainty ranging from 0.23 to 0.09 counts/s GBq ,respectively, with flood source thickness (from 12to200mm) at different source-to-detector distance (from SDD¼0.7 to1.1m). With the increase in source -to- detector distance, the extrinsic sensitivity decreases (e.g. from 121.36 to 118.77 counts/s GBq at source thickness ¼12 mm). The

reduction in the extrinsic sensitivity with increasing SDD is significant, beyond uncertainties. For example, at a flood source thickness of 12mm, the extrinsic sensitivity values were 121.29, 119.99 and 118.73 counts/s GBq, while the uncertainties were 0.23, 0.1and 0.15 counts/s GBq for SDD ¼ 0.7, 0.9 and 1.1m, respectively. Above results indicate that an increase in SDD is associated with an increase in extrinsic efficiency ; and a decrease in extrinsic sensitivity of both the extrinsic efficiency and the extrinsic sensitivity vs SDD for H¼ 12 and 200 mm, respectively. The results of this work indicate that instead of performing gamma camera QA using the common thin flood source, a thicker source would probably be more realistic. Such a source in corporate into account the effect of scattered radiation practically encountered when a patient is imaged using a gamma camera. It also shows that a source-to-detector distance equal to 0.967+/- $9X10^{-3}$ m represents a possible compromise for calculating the extrinsic sensitivity at areas on able counting efficiency in gamma camera QA tests.

Fernanda et al. (2010) designed and developed liver phantom has artifacts that simulate nodules and take different quantities, location and size and may also be mounted without the introduction of nodules. The objective of this study was to devoloped a liver phantom for quality control and training in nuclear medicine, and also may used specifically in spatial

resolution test of the gamma camera, also it permit simulation of expermints to evaluate changes in the image caused by source distance variation and to assist in the choice of image matrix size and the selection of the optimum energy window system in image acquisition. The design of this liver phantom simulator was based on models already in use in nuclear medicine, include, the whe design of this liver phantom simulator was based on models already in use in nuclear medicine, include, the multi Contrast / Resolution phantom and the Jaszczak phantom. The phantom consists of three 28cm -30 cm -2 cm a crylic plates and an a crylic plate of 28cm-30 cm-5 cm, hollowed out in the centre and with the geometry of an adult liver. The final thickness of the liver phantom is 9.0cm. For the tests, the researcher used two gamma cameras, the Elscint SP4 and Milleniuns MG. Simulations were performed using 90mTc diluted in water. Images for the analysis of simulated liver scintigraphy were obtained using a detector device located 5cm from the anterior surface of the phantom(Fig. 2). Usinga 32 _32 matrix size it was not possible to obtain diagnostic images. The higher the energy window, the greater was the loss of spatial resolution due to the detection of a larger amount of diffuse radiation, precluding observation of the nodules include din the phantom. Images obtained with a 64-64 matrix and an energy window of 5% enabled visualization of seven of the 32 nodules. Images obtained with an energy window larger than 5% showed greater

loss of resolution with a consequent reduction in imaged nodules. Using an image matrix of 128 -128 pixels with any acquisition window, it was possible to view nodules from 12.7mm in diameter; however, the quality of the image was poors. The best images were obtained with a matrix size of 256-256; the visualization of nodules with appropriate detection was possible with energy windows of 10 and15%. It is not eworthy that as the width of the energy window increased, the acquisition time decreased and wider spread Compton scattering was observed. by increasing the image acquisition time from 1 to 4 min, obviously the resolution improves, even with images acquired with 100 or 250 kcpm. However, it cause discomfort to patients because they need to stay longer immobilized. The results obtained for the phantom with nodules with a zoom of1,1.3,1.5and2.0 used the same matrix of 256 _256 in each image.The best resolution was obtained withthe1.3zoom.

Freek J et al. (2005) developed gamma camera with Charge-Coupled Devices (CCD) to evaluate the performance of a new device. The EMCCD used in this work is the CCD65 from E2V Technologies. It is a front-illuminated device with 288 lines and 576 pixels per line, and has an active area of 11.52 mm × 8.64 mm (20 μm × 30 μm pixel size). To reduce the dark current, the EMCCD is cooled to –50 ◦C, using a Peltier element. The researcher used a 1000 μm thick microcolumnar scintillator

module (CsI(Tl) FOS from Hamamatsu, type no. J6671), consisting of narrow CsI(Tl) needles (a few μm wide), grown on a 3 mm thick fibre-optic faceplate with fibres with a diameter of 6 μm, this scintillation module was coupled directly to the fibre-optic window of the CCD with optical grease; in the other set-up a fibre-optic taper with a taper ratio of 2.1:1 was inserted between the scintillation module and the EMCCD in order to increase the active area of the camera. The electronics board that drives and reads out the CCD is connected to a board containing a digital signal processor (DSP). An efficient photon-counting algorithm is executed on the DSP which detects and localizes scintillation events in real time by analyzing 50 entire CCD images per second. Spatial resolution measurements were performed for a Tc-99m source (140 keV, 37 MBq) and an I-125 source (about 30 keV, 37 MBq) using two tungsten blokes separated by a narrow slit (30 μm wide). Energy spectra of I-125, Tc-99m as well as a background noise spectrum were recorded. The influence of the number of scintillation events ('true counting rate') on the measured counting rate was determined by placing a Tc-99m point source at a distance of 28 mm from the CCD. A slab of lead with a hole of 2 mm at the centre was placed in front of the CCD. Different source strengths were obtained by natural decay. The maximum activity was 33MBq, and the 'true counting rate' was estimated by fitting a line to the straight part of the curve that is measured at low counting rates (30–230

counts cm−2 s−1). The result of this study determined that the Full Width at Half Maximum (FWHM) 99mTc 342μm and 270μm for 125I while the Full Width at Ten Maximum was 1123μm for 99mTc and 778μm for 125I. the energy resolution was estimated to be 24% FWHM (33 keV) for Tc-99m and 133% (36 keV) for I-125, the effects that an increasing event rate has on the fraction of scintillation flashes that can be detected, At event rates below a few hundred of counts cm−2 s−1, the number of detected events increases almost linearly with the true even rate, for Single Photon Emission Computed Tomography (SPECT) in which the number of detected count not exceed 1000counts the researcher estimate count losses to be only 2.1% and 3.8% at counting rates of 500 counts cm−2 s−1 and 600 counts cm−2 s−1, respectively, the counting rate effects occurring at much higher event rates, count losses at high event rates can be explained by overlapping of light flashes that occur in the CCD images, The number of detected photon interactions for the 35% window (140 ± 25 keV) in curves I–IV are 216, 1023, 2090 and 2623 counts cm−2 s−1, respectively.

Hosang et al. (2008) determined the detective quantum efficiency (DQE) of small gamma camera with three pinhole (1,2, and 4mm in hole diameter) and one-coded aperture (uniformity redundant array (URA), 286 holes, hole diameter 2mm) collimator, using Modulation Transfer

Function (MTF), normalized noise power spectrum (NNPS), and incoming signal to noise ratio (SNR). The researcher used small gamma camera that consist of CsI(Na) scintillation crystal (100mm in diameter, 3mm in thickness), a PSPMT (Hamamatsu R3292) with 28-X and 28-Y grid. The signal from PSPMT was amplified and digitized using ADC. Three pinhole 1,2, and 4 mm diameter was used. Coded aperture used was uniformly redundant array (URA) designed by Fennimore and cannon. The MTF was measured using 1mm diameter line source of 99mTc. The NNPS was measured with plane source (1mm in thickness and 50mm in diameter), the activity in the plane source was 8mCi of 99mTc at the beginning of the study. The DQE was calculated with incoming SNR2 defined as the number of photon incident onto the collimator. The solid angle from the plane source to the collimator was used to calculate incoming SNR2 value given approximately 3.75E+6 incident photon per cm2 for all pinhole. In the case of URA the researcher reduced the collection time to escape saturation. Thus, 4.69E+5 photon were incident onto the surface of URA collimator. The MTF value for 1mm pinhole is 0.93 at 0.6 lp/cm and 0.74 at 1.2 lp/cm for 2mm pinhole: 0.88 at 0.6 lp/cm and 0.58 at 1.2 lp/cm; for 4mm pinhole: 0.77 at 0.6 lp/cm and 0.31 at 1.2 lp/cm; for URA: 0.84 at 0.6 lp/cm and 0.48 at 1.2 lp/cm. The spatial resolution was inversely proportional to the diameter of the pinhole. Though each hole diameter of the URA is 2 mm,

it was observed that the spatial resolution of the URA was equivalent to that of the pinhole, 3mm in diameter. The MTF decrease was caused by scatter effect at many holes, URA. The DQE values of URA were much higher than those of all pinholes. The DQE ratio of URA to 2mm pinhole was about 8.1 at zero spatial frequency. Although MTF values of URA were a little lower than those of theoretical URA, higher DQE values were given by very low noise levels. The determination of DQE with MTF and NNPS enables the researcher to verify the total quality of gamma camera system quantitatively and effectively. Moreover, the DQE can be a useful design parameter to develop gamma-imaging systems.

Hosang et al. (2009) used the modulation transfer function (MTF) and normalized noise power spectrum (NNPS) instead of conventional NEMA slandered in the evaluate the performance of small gamma camera with changeable pinhole collimator using Monte Carlo simulation. For the acquisition of simulated gamma image, the small gamma camera used by the researcher was described by MCNP code. The energy of the gamma source was 140KeV which is the energy of 99mTc. The researcher used two kind of source geometry according to the NEMA standard, the one is a cylinder (30mm long; 1mm diameter), for the acquisition of line spread functions. The other is a disk (50mm diameter; 1mm thickness), for the acquisition of uniform flood images. Seven

collimators with 1.0, 1.5, 2.0, 2.5, 3.0, 3.5 and 4.0mm diameter pinhole were simulated using lead material of 3mm thickness. The FWHM values were measured in seven line images according to NEMA standard using Line Spread Function (LSF) acquisition and MTF computation. Sensitivity and differential uniformity were measured in seven uniform flood image according to NEMA standard using Region of Interest (ROI) definition, normalization, 2D NNPS computation and 1 D NNPS computation. MTF was inversely proportional to FWHM with person's correlation coefficient 0.995. the spatial resolution was described by the MTF of gamma camera system value for 1mm pinhole is 0.43 at 1 p/cm, 0.15 p/cm, 2mm is 0.40 at 1p/cm, 0.12 at 1.5 p/cm, 0.28 at p/cm and 0.02 at 1.5 p/cm. the average of MTF difference between 1 and 1.5 p/cm was 0.27 among seven pinhole collimator. NNPS was directly proportional to one of the sensitivities with Pearson's correlation coefficient 0.993. NNPS values For 1mm pinhole is 6.83E_4 at 1 l p/ cm and 2.22E_4 at 1.5 l p/cm for 2mm pinhole is 8.47 E-5 at 1lp/cm and 4.44 E_5 at 1.5 l p/cm and 4mm pinhole is 1.14E-5 at 1lp/cm and 4.64E_6 at 1.5lp/cm. The spatial uniformity of gamma camera system is basically related with pixel-to-pixel data fluctuations of output image data. Because sensitivity and differential uniformity only reflect statistical fluctuation and difference of two pixel data, the entire evaluation of spatial uniformity was given by only NNPS. In this study, the researchers have verified that

the spatial resolution of a gamma camera can be evaluated by the MTF as a function of spatial frequency. The NNPS of the gamma camera system enables the researcher to verify the total quality of the spatial uniformity.

Islamian et al. (2012) simulated a quality control Jaszczak phantom using SIMIND Monte Carlo and added the phantom as an accessory to the program. The researcher used the SIMIND Monte Carlo simulation program which is well established for SPECT with low energy photons for photonic physics and other applications, the program is freely downloadable from the related site: www.radfys.lu.se/simind, this program was originally designed for the calibration of Whole-body counters, but soon evolved to simulate scintillation cameras. It is now available in Fortran-90 and can be run on major computer platforms including PCs., SPECT Jaszczak phantom Deluxe which was specially design for high resolution camera, the phantom was constructed from Plexiglas material and consist of six spheres with different diameter (9.5, 12.7, 19.1, 15.9, 25.4, and 31.8) and 148 rods (4.8, 6.4, 7.9, 9.5, 11.1 and 12.7mm) used for measuring acceptance test and routine quality control of SPECT camera. The camera used in this study was E-Cam TM, Siemens Medical System. The phantom was filled with 370MBq ^{99m}Tc and image was acquired using 128 X 128 matrix, 128 views, 1.23 zoom factor, 3.9mm pixel size and images were reconstructed using

Butterworth filter. The SIMIND Monte Carlo code simulated the SPECT reconstructed image of the Deluxe model of SPECT Jaszczak phantom. The qualities of the produced image were compared in term of image contrast and spatial resolution. Image contract was calculated according to the methods describe by Toossi et al. (2010). The image contract of cold experiment phantom is 0.77, 0.62, 0.57, 0.37, 0.19 and 0.13 for sphere diameter of 31.8, 25.4, 19.1, 15.9, 12.7 and 9.5 mm respectively while the image contract for cold simulated was 0.66, 0.52, 0.48, 0.40, 0.23 and 0.20 for 31.8, 25.4, 19.1, 15.9, 12.7 and 9.5 mm respectively. The reconstructed spatial resolution of both SPECTs was nearly equal to 9.5 mm. Implementation of the SIMIND Monte Carlo program with the executable Jaszczak phantom file and also the related input file may be considered as a benefit, from the point of view of time saving and providing flexibility, for those who intend to plan a SPECT simulation study with the phantom. The researchers also suggest that the same phantom should be used for the simple assessment of X ray CT images and the assessment of image offset for SPECT/CT and PET/CT systems. Implementing such a phantom should provide a proper comparison of the assessment of

SPECT image performance more extensively practicable by experiment and simulated systems. In this work the researcher used high count acquisitions which result in slight ring artifact in the sphere image but this

artifact was not visible in the count statistics of the common clinical studies.

Staden et al (2007) designed and tested quality control phantom for gamma camera using standard inkjet printer. The ink used to print the phantoms was obtained by adding a well-mixed solution of black ink and ^{99m}Tc pertechnetate to the cartridge of a Hewlett-Packard inkjet printer (HP1220C), the cartridge was slightly modified by adding a tightly sealed plastic screw to accommodate easy filling of the cartridge, PowerPoint software was used to create an image that is representative of the radioactive distribution required, the distribution was then printed on paper (80 g m−2) using the radioactive ink, all radioactive phantoms were placed into a plastic sheath to prevent them causing any possible contamination, imaging was performed with a GE 400AT Starcam camera (General Electric Medical Systems, Milwaukee) fitted with a low energy all purpose (LEAP) collimator and IM512P acquisition software (Alfanuclear SAIYC, Buenos Aires). The amount of ink deposited per unit area and the amount of activity added to phantom was measured. The uniformity of the camera was determined by measured the integral (IU) and differential uniformity (DU) for five printed radioactive flood source with 1200MBq ^{99m}Tc deposit in every sheet and using 64X64 matrix size. For comparison, the camera uniformity was also determined using

National Electric Manufacture Association (NEMA2001) protocol with ^{57}Co flood source and (IU) and (DU) were measured. System spatial resolution was evaluated using two lines (1mm thick) printed 10 cm apart and two other printed perpendicular to the first, the paper was imaged at 10cmm distance from detector with 512X512 matrix, also for comparison camera resolution was evaluated using NEMA2001 protocol using two capillaries tube, more, the four quadrant bar phantom was used to evaluate camera resolution. Result of this study showed that (IU) and (DU) obtained with NEMA method (^{57}Co) for Useful Field of View (UFOV) was 4.11 and 2.68% respectively, the IU of Central Field of View (CFOV) was 2.10% while he IU of CFOV for printed source was 2.29+/-0.67%, the average DU of ^{57}Co source was 1.50% and for printed flood source 1.50+/-0.23%. The average Full Width at Half Maximum (FWHM) of printed phantom was 10.1 and for NEMA phantom was 10.5 while the average Full Width at Ten Maximum (FWTM) was 17.7 for printed source and 18.3 for NEMA source. The two image of bar phantom was visually very similar. Even the slightly different between the result of printed phantom and NEMA, the results were still acceptable when compared to accepted values of NEMA protocols.

Lees et al. (2011) developed small gamma cameras based on scintillator coated charge coupled device (CCD) technology that was originally developed for use in X-ray astronomy, this Communication describes the development of a prototype high resolution small field of view mini gamma camera that would be highly suited for intraoperative imaging. This new type of gamma camera has been designed to offer high spatial resolution imaging (- 1 mm, using a pinhole collimator), appropriate for medical and veterinary applications, which consists of a CCD, a CsI(Tl) scintillator and a pinhole collimator, the CCD to pinhole distance is fixed at 10 mm. The distance from the pinhole to the object being imaged determines the demagnification on the CCD. Lead shielding around the sides and back of the detector enclosure minimizes image

degradation from scattered photons and background radiation. Single pin hole collimator was used, two collimators, with pinholes of 0.5 mm and 1.0 mm diameter, were manufactured (Ultimate Metals) from tungsten discs, 6mm thick and 45 mm in diameter, each having an acceptance angle of 60 degrees. As part of new camera development a CsI(Tl) columnar scintillator (600 mm thick on an amorphous carbon substrate) from Hamamatsu was coupled directly to the CCD with Dow Corning optical grease. The Mini Gamma Ray Camera (MGRC) has been designed to be sensitive over the energy range 20–140 keV. The CCD was cooled using a Melcor thermoelectric device with a finned forced-air

heat sink, the camera housing being evacuated to prevent condensation on the CCD. The operating temperature of the device was approximately -10ºC. The photons generated in the scintillator by the gamma rays are collected in the CCD and converted to charge in the image area during the integration time period. This charge is transferred to the store sections then into the readout register. Following transfer through the readout register, the charge is multiplied in the gain register before conversion to a voltage by a large signal output amplifier. The software used in this new camera were combined from different algorism which are multi-scale algorithms, automatic scale selection and Scale-Space Theory, and are used in a wide range of image analysis applications: detection of lung nodules, quantifying complex landscapes and blob analysis. The resulting spatial resolution of MGRC was less than 1mm after measured the Full Width at Half Maximum (FWHM). For real patient which was injected with 600MBq ^{99m}Tc-HDP, the indicated activity of the order of 200kBq within the imaged area, this would equate to about 0.03% of the amount of activity initially administered to the patient 3 hours previously, since this represents a relatively low count rate, some background activity can be seen around the uptake due to scattered photons arising from the body of the patient, this may be due to the sub-optimal shielding around the camera body. At the end the use of this small highly collimated probe systems for intraoperative and intensive care applications. These have

been used for a wide range of applications with particular emphasis on identifying the uptake of radiopharmaceuticals in tumors during surgical operations. By injecting a radiopharmaceutical that selectively concentrates in tumor tissue, it is possible to identify sites of increased uptake of radioactivity. This allows the surgeon to identify the focal uptake of the tracer in lesions, thus aiding the identification of tissues requiring surgical removal.

Ejed et.al (2011) Assessed gamma camera intrinsic uniformity in developing country with unstable power supply environment .the camera used in this study was the Siemens e.cam (signature series) SPET system with single head (Siemens Medical Solutions U.S.A, Inc.) which was installed at the center(Nigeria) in March, 2006. The camera set up for the flood uniformity test is as in Figure 1. A point source of technetium-99m pertecnetate (99mTcO-4) of activity ranging from 0.74MBq to 3.7MBq was used each time the test was performed. A small piece of cotton wool was placed in the vial and drops of 99mTcO-4 were placed on the cotton wool while trying not to exceed the cotton's saturation capacity. The collimator was removed and the detector was fully retracted with the gantry rotated so that the detector was at 0oC. The integrated source holder was extended from its storage position on the rear bed and pulled until the source holder was approximately centered. The prepared point

source in the vial was clamped, with the capped end of the vial, into the source holder making sure that the cotton tip with the activity was approximately centered above the detector. Thirty million counts were acquired using a matrix of 1024X1024 and a zoom factor of 1.0 (these parameters were automatically preset by the camera) after the camera had been peaked for 99mTc i.e. its energy discrimination window adjusted to be centred on the photo peak of 99mTc. The researchers obtained 143 reading of camera intrinsic uniformity and the result showed that The integral uniformity for the CFOV lied between 3.43% and 1.49% against the acceptance test value of 3.29% while the integral uniformity for the UFOV lied between 4.51% and 1.9% as against 5.21% for the acceptance test. The differential uniformity for the CFOV had values between 1.99% and 1.04% against acceptance test value of 2.25% while that of the UFOV had values between 2.84% and 1.23% against 2.63% for the acceptance test. The shortest time the camera was on before the intrinsic flood uniformity test was performed was 15min and the test produced a flood uniformity of 2.27% and 2.32% for the integral uniformity for CFOV and UFOV, respectively. The differential uniformity for the same test was 1.34% and 1.34% respectively for the CFOV and the UFOV. These result showed that the uniformity of the gamma camera under this condition is within an acceptable range for both planar and SPET imaging.

Kazuki et.al. (2008) developed a balloon borne electron. Tracking Compton camera for sub-MeV to MeV gamma ray astronomy. The researcher used scintillation camera that consist of Hamamatsu 64-chanel multi anode sensitive photomultiplier tube (OSPMT-H8500), a pixilated scintillator array (PSA), and a GSO(Ce) (GD_2SiO_5.Ce) crystal that has advantage of a much smaller dead space and a larger effective area. In addition a read out system with low power consumption (≤ 2W/64chanel) was used because the researchers need 108 scintillation camera corresponding to 6912 channels. The read out system used was ASIC chips, VA32-HDR11 produced by IDEAS with 147mW/64chanel and a dynamic range of 35pC. The researcher irradiate the GSO(Ce)PSA with 662KeV gamma ray from a 1 MBq 137Cs source at a distance of 30cm. for energy calibration different source of energy was also used including 54Mn, 57Co, 22Na and 133Ba. The researchers investigate the relation between the resistance and the attenuation factor. The result of the minimum to maximum gain ratio of the 662KeV peak value is 1:1.9 +/- 0.3 (RMS), and the measured ratio with the attenuator board is 1:1.6 +/- 0.1 while the energy resolution at 662 KeV is 10.6% FWHM These are fit to DE/E(FWHM) ¼ 10.670.6(E/662

[keV])_0.4970.03, where fit parameters are given with RMS errors in the range from 31 to 835 keV. The measurable energy dynamic range of the

system is about 30–900 keV at all 64 pixels. These results show that the system of the scintillation camera with the attenuator board performs adequately with good energy resolution and a wide dynamic range with low power consumption. As a result, the researcher obtained good energy and position resolutions and a wide energy dynamic range of the scintillation camera with low power consumption. The performance of the system is sufficient for use as a Compton-scattered gamma-ray camera for balloon experiments. We have been constructing a Compton camera to be used with this system and testing its performance.

Koike et al. (2011) developed a prototype gaseous gamma camera with a Gas Electron Multiplier (GEM) for medical application in order to increase the spatial resolution of old anger camera. The system consists of three devices: a detector, an Ethernet hub, and a PC. The detector consists of a GEM-chamber and integrated readout electronics. The GEM chamber, which consists of three parts: a converter, an amplifier, and a read out component. The gamma-ray converter consists of four gold-plated GEM foils and a gold-plated cathode. Each converter converts incoming gamma rays into electrons. Both surfaces of the GEM foil are plated by gold, with which gamma rays interact easily because of its large atomic number. a liquid crystal polymer (LCP) was used. The readout electronics are integrated into the detector and linked to a PC with an

Ethernet connection. All signals from the readout strips are processed and transferred to the PC as event data. The readout module consists of an ASIC and an FPGA. The ASICs processes analog signals and the FPGA processes digital signals. Researcher developed a simple application program for data acquisition; the program runs on Linux OS and has a number of Graphical User Interfaces (GUIs). In order to test the performance of new prototype camera, researcher conducted several measurements using a phantom filled with 99mTc (141 keV) as the radioactive source. The measurements with pinhole collimator, the distances between the radioactive source and the collimator and between the collimator and the detector were both 100 mm, respectively, and imaging was performed with a pinhole collimator of 2mm in diameter. The efficiency of gamma-ray-detection for a 141 keV gamma ray at a stable operating voltage (4900 V) was 2:57_0:05%. On the other hand, the efficiency calculated by the GEANT4 simulation was 2:78_0:02% for a similar detector setup. This indicates that we achieved a detector setup with sufficient effective gas gain. The relationship between radioactivity and acquisition count was linear. The Full Width at Half Maximum (FWHM) was measured and within the acceptable limits. Gamma camera with GEM provides spatial resolution of 2-3mm compared to 6-10mm for old anger gamma camera.

Lees et al. (2010) investigated the use of high resolution mini-phantoms for the evaluation of planar imaging devices with spatial resolution of the order of 1 mm. the researcher have developed a new type of gamma camera that offers high spatial resolution imaging (-1 mm, using a parallel hole collimator), highly appropriate for medical and veterinary applications Lees et al. (2010). The simplest form of the mini phantom was a three- hole design in a piece of Perspex 5 mm thick with one large hole, 3 mm in diameter and two other holes of 2 mm in diameter on 5 mm perpendicular spacing. The researchers used the concept of the ‘‘WilliamsPhantom’’, they designed1 two high resolution (HR) phantom s giving the option of having ‘‘hot’’ spots or a uniform source with ‘‘cold’’ spots’’. The first HR mini-phantom has four holes, 4, 3, 2 and 1 mm diameter drilled in a piece of Perspex 12 mm thick. The second phantom had four pins with diameters 4,3,2 and 1 mm with the same spacing as the ‘‘hole’’ version. All imaging was undertaken in the Medical Physics Department at Queen’s Medical Centre using the high resolution gamma camera. All images were recorded in frame mode and stored on a dedicated personal computer. A fine bore hypodermic needle, 0.5 mm diameter and 25mm long (25G_100) commonly found in nuclear medicine depart ments , was used to fill the HR four hole phantom with liquid Tc-99m pertechnet ate obtained from the radiopharmacy unit in Medical Physics. Visualisation of such small volumes of clear radioactive

solution presented potential problems with spillage of small drops resulting in contamination. A ddition of a small amount of dye (food colouring) made the process of filling the phantom and visualization of any accidental spillage easierto observe. Subsequent use of a 200 ml air displacement micro pipette Pipetmans enabled accurate filling of the hole sin the mini- phantom with calibrated amounts of radioactive solution. The three-hole phantom was filled from a 1 ml stock solution containing 388 MBq of ^{99m}Tc (the small total volume of the holes resulted in an overall phantom activity of -3.4 MBq). The phantom was placed 13 mm above the camera and was imaged for 18 min (-200 counts per second). Initial attempts at phantom imaging showed ir regular distribution of a ctivity within the holes. Although the 3mm diameter hole was completely filled, on closer inspection the two smaller 2mm diameter holes contained air bubbles and an uneven distribution was seen in early gamma camera images. After modification of the filling procedure consistent uniform filling of the smaller holes was achieved. The three holes can be clearly visualised. The slice through the two small holes (on 5mm pitch) shows clear separation. The spatial resolution at FWHM was calculated to be 0.9 mm, slightly less than the theoreticalon-axis spatial resolution of 1.2 mm expected from the detector geometry and single pinhole collimator (Mettivier etal.,2003)

Holstensson et. Al (2010) experimentally measured the effect of energy and source location on gamma camera intrinsic and extrinsic spatial resolution. The two main factors that determine the spatial resolution of a system are (i) the collimator design and (ii) the accuracy with which scintillation events can be localized, which is limited by statistical variation in the number of scintillation photons produced. Although a value for *R*intrinsic is typically measured as part of the clinical acceptance testing of a gamma camera for the radionuclide 99mTc, *R*intrinsic varies with photon energy . A different value of *R*intrinsic is therefore required for accurate simulation of each different radioisotope and photon emission energy. Experimental images were acquired on a dual-head 9.5 mm NaI(Tl) crystal Philips FORTE and a dual-head 15.9 mm NaI(Tl) crystal Philips SKYLight gamma camera (Royal Philips Electronics, The Netherlands). Both cameras were equipped with 55 PM tubes arranged in a hexagonal array and with a rectangular FOV measuring 38.1 cm in the *x*-direction and 50.8 cm in the *y*-direction. For anterior–posterior images, the *x*-direction corresponds to the cranio-caudal axis and the *y*-direction corresponds to the mediolateral axis in the patient frame.the result demonstrates the improvement in *R*exp intrinsic as a function of energy of the photons being imaged for the thin crystal camera. The improvement in *R*exp intrinsic from 99mTc (140.5 keV) to 131I (364.5 keV) is 21% for the thin crystal and 17% for the thick crystal.

The measured *R*exp intrinsic values for both the thin and the thick crystal cameras are 2.66+/-0.07,2.54+/-0.07,2.23 and 2.1 +/-0.1mm for 140.5 ,171.3, 245.4 and 364.5 KeV simultaneously for thin crystal and 3.1+/-0.1 ,3.0+/-0.2 , 2.9+/-0.2 and 2.6+/-0.2 for 140.5 ,171.3, 245.4 and 364.5 Kev simultaneously for thick crystal.the result also shows The calculated profile widths of the line and maximum pixel count rates in the images of the sphere created using energy-dependent *R*electronics 0.00mm values for FWHM are 7.18+/-0.06 ,10.6+/-0.1 and 15+/-0.3 mm for 1cm ,5cm and 10cm depth of source simultaneously and *R*electronics 1.55mm values for FWHM are 7.45+/-0.03 ,10.8+/-0.1 and 15.2+/-0.3 mm for 1cm ,5cm and 10cm depth of source simultaneously and *R*electronics 2,49 mm values for FWHM are 7.84+/-0.07 ,11.1+/-0.1 and 15.4+/-0.3 mm for 1cm ,5cm and 10cm depth of source simultaneously

Coca Perez et.al. (2008) established a national program for the quality control of nuclear medicine instrument in Cuba and was certified and approved by the regulatory authorities. The program was developed the national Cuba guidelines for a set of standardized and uniform quality control procedure taking into account the technical features of the local instrumentation and the availability of local resources such as phantom. These protocols were based on international publication such as IAEA and NEMA. The documents include the quality control of dose calibrator,

directional detectors and well counter, planner gamma camera, SPECT system, whole body system and interface system. The program establishes official regulations and audit service, set-up educational activities, distributes technical documentations, and maintains a national phantom bank, constitutes valuable and useful tools to guarantee the quality of nuclear medicine instrumentation. A national course on the quality control of nuclear medicine instrumentation was organized and established, it is main objective was to educate and trains the persons responsible for carrying out these tasks in each nuclear medicine department in Cuba, the course was registered at the National College of Health, including forty hours of theory and practical. A data base was created of phantoms and accessories available within the Cuba for quality control of nuclear medicine instrumentation, the data was organized at the web site www.sld.cu/phbank/nmphincu.htm, and the program organized the share of quality control phantom between the Cuba nuclear medicine centers and hospitals by delivered the required phantom to the center according to their need. An audit service licensed and registered by the Centro National de Seguridad Nuclear (National Center of Nuclear Security) was organized and created. The role of the audit service is to annually assess the state of the instrumentation in all nuclear medicine departments within the country and to evaluate compliance with the quality control programs. More than 10 inspections have been performed

by the CCEEM to date and have been useful in improving the quality control programs for nuclear medicine instrumentation. Finally, measurements were performed in situ in all the national nuclear medicine services to evaluate the current state of gamma-cameras and SPECT systems. The selected tests and procedures were based on the nuclear medicine instrumentation quality control program previously established. The 5 gamma-cameras and 5 SPECT systems in the country were evaluated for uniformity, spatial resolution, sensitivity, energy resolution, linearity, and tomographic uniformity, center of rotation, tomographic resolution, and total performance .

Jeong et. al.(2004) improvement the performance of small gamma camera using NaI(Tl) plate and position sensitive photomultiplier tube (PSPMTs) and check the camera performance before and after correction methods applied. The camera used in this study was small gamma camera consisted of a general purpose parallel hole collimator (24 mm in length, with a hole diameter of 1.5 mm and a septum thickness of 0.2 mm), a scintillation crystal (NaI(Tl) plate, 120 mm in diameter and 6 mm in thickness), a 5 inch PSPMT (Fifty-six signals from the R3292 PSPMT were reduced to four signals, the four signals were amplified and digitized using ADC with 40 Msamples s−1 sampling rate then used to localize an event employing the Anger logic), the data acquisition

programs were based on Kmax. Position mapping correction developed in order to correct the distorted hole position on the image obtained by scintillation crystal using A lead hole mask (150 mm × 150 mm × 4 mm, 1 mm hole diameter, 5 mm pitch) placed in contact with the NaI(Tl) plate crystal without a collimator, and acquired images at different distance (0, 0), (2.5 mm, 0), (0, 2.5 mm) and (2.5 mm, 2.5 mm). Energy calibration was performed using the pulse height spectra obtained from each hole position, obtained for 10 hours using a point source (2 mCi 99mTc) located 40 cm above the detector. Flood correction was performed using uniformity correction table. Spatial resolution was measured using two capillary tubes having 50 μCi 99mTc each with inner diameter measurements of 0.4 mm, Full width at half-maximums (FWHMs) of the profiles of the two-line images were measured. Linearity was measured with a parallel-line bar phantom, and was expressed as a standard deviation of the line spread function peak separation, then the linearity was calculated using the line image. The uniformity was measured using a uniformity phantom that was filled with radioactive solution (500 μCi 99mTc), and integral uniformity and differential uniformity were also measured. In order to comparative NaI(Tl) crystal result, CsI(Tl) plate was applied to the camera and checked the performance at the same parameter as NaI(Tl) images acquired. The result of this study showed that the resolution of the NaI(Tl) plate system was improved by about

16% using the correction method, and was similar to that of the CsI(Tl) array system after correction, FWHM improved 6.7mm to 3.2 after correction at 30mm distance. The sensitivity of the NaI(Tl) plate system at the centre of the FOV remained similar both before and after correction , however, the sensitivity of the NaI(Tl) plate system at 30mm off-centre considerably increased after correction, from 0.7 cps μCi−1 to 2.0 cps μCi−1, the sensitivity of the NaI(Tl) plate system was considerably better than that of the CsI(Tl) array system over the entire FOV after correction (NaI(Tl) plate: 3.4 cps μCi−1, CsI(Tl) array: 1.4 cps μCi−1 at the centre. The linearity of the NaI(Tl) plate system improved after correction, from 0.5 mm to 0 mm at the centre of the FOV, and from 1.5 mm to 0 mm, at 35 mm off-centre. Before correction, the linearity of the NaI(Tl) plate system was slightly worse than that of the CsI(Tl) array system, but after correction the linearity of both systems was about the same. The integral and differential uniformity of the NaI(Tl) plate system both improved after correction, from 9.7% to 5.2% and from 3.6% to 2.1%, respectively. The uniformity of the NaI(Tl) plate system was better than that of the CsI(Tl) array system after correction.

Holen et.al. (2008) assessed the quality of an image obtained with a rotating slat (RS) collimator in comparison to classical projection image

obtained using parallel hole (PH) collimator. the methods used in this study was Monte Carlo Detector Model ,the researcher used also Geant4 application for tomographic Emission (GATE), it was used to model both the RS and the PH collimated camera. The detector was the same for both systems and was modeled as a pixilated solid state detector consisting of 192X192 individual CdZnTe crystals. The surface of one pixel is 1.8 mm × 1.8 mm while its height was set to 5 mm. To make the efficiency of the detector independent of the collimator type, the active area of one pixel is set to be only 1.5 mm × 1.5 mm, allowing the collimator to have septa of 0.3 mm thickness. The active area will thus be independent of the collimator type since the area covered by the collimator coincides with the inactive detector area. The RS collimator was simulated as 193 parallel lead slats of height 40 mm, placed in between two detector pixels rows. The thickness of a slat was set to 0.3 mm while the length was equal to the length of the detector; being 345.6 mm The PH collimator had the same height and thickness as the RS collimator (40 mm) and was matched to the pixilated detector. This resulted in a parallel hole collimator with square holes of 1.5 mm × 1.5 mm. The RS collimator/detector pair was rotated around its own axis in 128 discrete steps at a speed of 20 s per rotation. The PH collimator/detector pair did not move during simulation. The reconstruction of the plane integral data to projection images was performed using a MLEM algorithm the PH

projection images were deconvolved using the Richardson–Lucy method in order to make a fair comparison, also Contrast to Noise Ratio (CNR) was obtained using classical methods of gamma camera .the object size was measured as Point Spread Function (PSF).and also image of MCAT phantom was taken in which MCAT simulate the bone scan which is very wide spread nuclear medicine scintegraphy. The result of this study showed that cold spot contrast recovery is worse for the RS collimator and the differences becoming larger as the cold lesion become smaller an increased contrast recovery can however be obtained for the hot spot this improvement is larger as the hot lesion become larger. The CNR for 9 , 12 mm hot spot is six ,ten times larger respectively ,the PH collimator has a better resolution ,the RS collimator in avery small low contrast and this situation however different when considering more realistic with larger lesion or high contrast . The RS collimator appeared relative improvement when the lesion become larger the improvement is 34% for 6mm lesion and 54% for 10mm lesion.

S. BAECHILER et.al (2008) measured the feasibility of gamma camera acceptance test for different manufacture but all these cameras are introduced by the SWISS Federal Office of Public Health found on Switzerland. Three types of cameras used in this study which are a single

head system (Millennium – General Electric - USA), a two head system (E.Cam - Siemens - Germany) and a three head system (Triad - Trionix – USA) with NEMA (National Electrical Manufacturers Association) - NU-1, 2001 and/or IEC (International Electrotechnical Commission) 61675-2, 1998. Intrinsic homogeneity was done with appoint source without collimator placed in lead box with copper filtration of at least 2mm at distance higher than 5 times useful field of view (UFOV) of the camera, the count rate should not exceed 20 Kcps with pixel size 6.4mm +/-30% and contain at least 10,000 events these measurements applied for both UFOV and central field of view (CFOV). Intrinsic spatial resolution and geometrical linearity also measured with 3 mm thick lead plate with 1 mm slits spaced by 30 mm, covering the whole surface of the camera, the Line Spread Function (LSF), Full Width at Half Maximum (FWHM) and Full Width at Ten Maximum (FWTM) were measured. Spatial resolution and system sensitivity also detected by use two capillaries <1mm filled with Tc-99m and placed on a Styro foam at 10 cm of the collimator and FWHM and FWTM were measured. Intrinsic energy resolution done using 2 point source Co-57 and Tc-99m placed successively in front of head of camera with counting rate not exceed 20Kcps, and the photopeak spectrum were measured with FWHM for two different energy. Behaviour of the counting rate according to the activity with scattered radiation for every camera was done using PMMA cylinder phantom

filled by 10GBq of Tc-99m, and recorded activity when the count rate decreased by 20% of the expected value. The result of this study showed that the integral uniformity% of UFOV is 3.00, 7.15 and 10 and the CFOV is 2.37, 5.75 and 2.03 for E.cam, Millennium and Triad respectively. Also the result showed that the FWHM (mm) for linearity was 3.9, 4.2, and 4.2 and FWTM is 7.4, 8.3, and 8.0 for E.cam, Millennium and Triad respectively. The sensitivity (count.s-1.MBq-1) of the cameras is 33.0, 30.9, and 54.7 for E.Cam LEHR, Millennium LEHR and Triad LEGP respectively. The count rate (Kcps) of E.Cam camera is 84.3, for Millennium camera is 110 and 48.1 for Triad camera while the dead time (μs) for Millennium camera is <3.3, 4.4 for E.Cam camera and 7.6 for Triad camera.

Yamamoto (2010) developed and tested a small field of view (FOV) gamma camera using s new $LaBr_3$ (Ce) scintillator. The gamma camera developed consist of a 2mm thick $LaBr_3$ (Ce) scintillator (Saint Gobain, BrilLanCe 380, USA) and a 25.4mm (2in) square multi-anode PSPMT (Hamamatsu H8500, Photonix, japan). The $LaBr_3$ (Ce) scintillator was directly coupled to the PSPMT by it is manufacture and was contained in a hermetically and light sealed aluminum case. The detection efficiency of 2mm thick $LaBr_3$ (Ce) for ^{99m}Tc gamma photon (141KeV) was around 40%. The size of $LaBr_3$ (Ce) is 50.8mm X 2mm and the upper side was

covered by a white reflector while the other side was painted black to reduce the stray light in the scintillator. The thickness of the aluminum case was 0.5mm. The size of the detector is 58mm X 58mm X 32.5mm. The signal from PSPMT was read out by 64 coaxial cable and fed to the gain control amplifier, the output from amplifier were fed to weighted summing amplifier and digitized by 100MHz free running AD convertor. Energy resolution were measured without collimator using ^{57}Co and ^{241}Am which result was 8.9 % Full Width at Half Maximum (FWHM) for Co and 13.4% FWHM for Am. The intrinsic spatial resolution was measured using a 2mm thick tungsten slit phantom with 1mm slit positioned on the detector, the result showed for ^{57}Co was 0.75 mm FWHM and 1.4 mm FWHM for ^{241}Am after correction applied. Sensitivity was measured for the camera using 50μCi point source with less than 1 mm size, the source was positioned in front of the pinhole collimator and the count rate was measured by changing the distance between collimator surface and the point source in 5 mm step from 0 to 30mm, the result of sensitivity was 0.0047% at 10 mm and 0.0017% at 20 mm from the collimator surface. The image quality in the corrected mode was measured using several phantoms but the result was assessed visually showed. The flood image, shows good uniformity and has no observable system non-uniformity. Flood images of Co-57 measured at approximately two month and two years after the fabrication , The flood

image showed significant distortion due to the change in LaBr3(Ce) of its hygroscopic characteristic . Almost half area of the FOV produced no signal.

Sokole et al. (2010) recommended some procedure for quality control of nuclear medicine instruments. After installation, and before it is put into clinical use, a nuclear medicine instrument must undergo thorough and careful acceptance testing, the aim being to verify that the instrument performs according to its specifications and its clinical purpose. Once the instrument has been accepted for clinical use, its performance needs to be tested routinely with simple QC procedures that are sensitive to changes in performance. Records of test results should be kept in a log-book or digital record. The routine test for planer gamma camera includes 1- Physical inspection, the purpose of the test is To check collimator and detector head mountings, and to check for any damage to the collimator and must be carried daily (Inspect for mechanical and other defects that may compromise safety of patient or staff; if collimator damage is detected or suspected, immediately perform a high-count extrinsic uniformity test). 2- Collimator touch pad and gantry emergency stop To test that the touch pads and emergency stops are functioning, the frequency of the test is Daily (Both the collimator touch pads and gantry emergency stop must function if there is an unexpected collision with the

patient or an obstacle during motion; the touch pads must be checked each time the collimators are changed). 3- Energy window setting for ^{99m}Tc to check and centre the preset energy window on the 99mTc photopeak, should be done daily (The test is intended to check the correct ^{99m}Tc energy window). 4- Background count rate to detect radioactive contamination/excess electronic noise an performed daily (The background count rate should be stable under constant measuring conditions). 5- Intrinsic/extrinsic uniformity and sensitivity for ^{99m}Tc (or ^{57}Co) – visual To test the response to a spatially uniform flux of 99mTc (or ^{57}Co) photons, for uniformity and overall sensitivity and must be carried daily (Visually inspect either an intrinsic or extrinsic (whichever is most convenient) low count uniformity acquisition; if intrinsic method is selected, each collimator must be checked periodically by an extrinsic uniformity test (preferably with high-count acquisition); record the cps/MBq to check and monitor sensitivity). 6- Intrinsic/extrinsic uniformity and sensitivity for ^{99m}Tc (or ^{57}Co) – quantitative- To monitor the trend in uniformity with quantitative uniformity indices, and to check the sensitivity, may be carried weekly or monthly. 7- Spatial resolution and linearity – visual- To detect distortion of spatial resolution and linearity carried monthly or each Six-monthly(Visual-quadrant bar or orthogonal hole pattern; intrinsic or extrinsic, depending on convenience;

if an orthogonal hole pattern is used, the results can be quantified if special software is available).

Sven-A et al. (2005) evaluated the performance of gamma camera using detective quantum efficiency (DQE). The use of DQE related to measure of Point Spread Function (PSF), Line Spread Function (LSF), Full Width at Half Maximum (FWHM), Modulation Transfer Function (MTF), Signal to Noise Ratio (SNR) and Normalized Noise Power Spectrum (NNPS). This study was made on a Siemens ECAM gamma camera with a 3⁄8inc crystal and an ECAM+ gamma camera with a 5⁄8inc crystal, both with rectangular detectors. All purpose and high resolution parallel hole collimators were used. The intrinsic spatial resolution was 3.9 mm for the ECAM camera and 4.6 mm FWHM for the ECAM+ camera. The system planar sensitivity was about 10% higher for the ECAM+ camera. The MTF of a gamma camera was measured with a 1 mm diameter line source. Uniform images were acquired with the same collecting time per activity unit with a NEMA (National Electrical Manufacture Association) sensitivity plane source (NEMA 1994). The plane source, 1 mm thick and with a diameter of 100 mm, was filled with 99mTc. The measurements were made in a water tank at 2 cm and 12 cm depth. Measurements were made with ^{99m}Tc, using three different pulse height windows 103– 154

keV (40%), and 126–154 keV (20%) and 132–154 keV (15%). The activity in the plane source was at the beginning of the measurement series 123.7 MBq and at the end 87.2 MBq with a collection time between 90 s and 128 s. From the line source images the tails of the LSF were extrapolated exponentially (Extrapolation levels between 1% and 0.1% of the maximum of the LSF were used) then the MTFs were calculated by Fourier transformation of the LSF, from calculated MTF and normalized noise power spectrum calculated from uniformity Images the noise-equivalent quanta were calculated, lastly DQE was calculated with SNR. Measurements showed that the 40% energy window had a high DQE compared to the other energy windows for frequencies up to about 0.03 cm−1 at 12 cm depth and for frequencies up to about 0.07 cm−1 at 2 cm depth, At 12 cm depth, 15% window was preferable for frequencies over approximately 0.05– 0.07 cm−1 for both the HR and AP collimators, The AP collimator was found to be superior for frequencies below 0.4–0.5 cm−1, while the HR collimator was superior for frequencies over 0.5 cm−1, Measurements at 2 cm showed that the AP collimator and a 20% window was best for all frequencies of clinical interest (<1.2 cm−1), for frequencies exceeding 0.6 cm−1, window widths of 20% and 15% gave almost identical results. A difference was found in DQE between the two crystal thicknesses, with a slightly better result for the thick crystal for measurements at 12 cm depth, At 2 cm

depth, the thinner crystal was slightly better for frequencies over 0.5 cm−1. The thicker crystal gave higher values for DQE, whereas when the organ was near the collimator surface the thinner crystal was slightly better especially for the AP collimator at frequencies over 0.5 cm−1. The system spatial resolution for the HR and AP collimators was 7.4 mm and 9.4 mm FWHM at 10 cm and about 0.4 mm higher, respectively, with the thick crystal. The difference in spatial resolution between the crystals was smaller and about 0.2 mm when measured with scatter. The difference in sensitivity between the collimators is about 65%. In nuclear medicine examinations using 99mTc and when the organ of interest is at greater depths in the body, a 15% window, compared to a 20% window, results in a better contrast and improved MTF curve due to rejection of scattered radiation.

Fidler et al. (2001) upgraded analog gamma camera with digital acquisition system with PC based system from International Atomic Energy Agency (IAEA) and ministry of science and technology of Slovenia, several national research groups were involved in the IAEA development project for the acquisition card with software and the standard set of clinical protocols from China, India, Cuba, and Slovenia, upgrading involved development of acquisition card by using ISA format

acquisition card, solution for adjusting amplitude and timings for input signals from a variety of gamma Cameras, acquisition driver incorporated in PIP (Portable Image Processing), on-line energy and count correction of image data, stable function of the system for all kind of possible clinical studies (fast and slow dynamic, static, gated and combined studies), continuous upgrading. Also the software was developed using MSDOS operating system in WINDOWS (3.1, 95, 98), PIP system for patient database and general data processing, tools for end-user development of clinical protocols (C++ library, macro functions) , algorithms for automatic analysis of clinical data with possible manual intervention, tools for image, dynamic curves and ROI processing, images from study analysis in standard picture formats (i.e. PCX, BMP), set of gamma camera quality control functions (NEMA tests), converter to and from "Interfile" format, SVGA color scale for display, results of analysis on one page, printing of documents in high spatial resolution (1200x1200 dots/inch) and on low cost high quality media (paper, transparencies), archiving the original image data and reporting documents on low cost CD as "soft" copy, network support. The acquisition system developed mainly depending on three universities project, first Acquisition card from Bombay Nuclear Research Institute with signal′s gain and offset control, AD conversion, energy correction, creating images and gate control, second Acquisition card from Havana

University Institute with signal`s gain and offset control, AD conversion with saving the position, energy and other control data (i.e. gate signal, signal for gantry control) are transferred to the computer`s memory using PORT transfer, the third one is Acquisition card from Ljubljana University Medical Centre with signal`s gain and Offset control, time control, AD conversion, saving of position, energy and all other control data for each detected gamma event by computer`s PORT transfer to the computer memory. The project applied for 300 gamma cameras spread over 52 developing countries. The Slovenian system GAMMA-PF is the most adequate, due to better technical performance, stability of functioning, facility of installation, technical support, lower price, accomplishing in delivery rime schedules and professionalism of the involved team

Zanzonico (2009) reviewed the quality control procedures for nuclear medicine instruments. Nuclear medicine is critically dependent on the accurate, reproducible performance of clinical radionuclide counting and imaging instrumentation. Gamma camera is the most widely used imaging device in nuclear medicine. The performance parameters most commonly evaluated as a part of routine gamma camera quality control program include uniformity, spatial resolution, spatial linearity, and energy resolution and peaking. Gamma camera uniformity may be

evaluated either intrinsically (without collimation) or extrinsically (with collimation). Intrinsically, a point source (□1mL in volume and containing about 18.5 MBq) of ^{99m}Tc placed 5 crystal dimension from and centered over the uncollimated detector. Extrinsically, a uniform flood, or sheet source (typically 185- 555MBq) of ^{57}Co or ^{99m}Tc placed directly on the collimated detector. In both intrinsic and extrinsic type of uniformity a total of 10-15 million count is acquired and uniformity quantities for integral uniformity (maximum count per pixel – minimum count per pixel / maximum count per pixel + minimum count per pixel X100%) and differential uniformity (same equation of integral put applied for every 5 pixels segment in every row and column of the flood image). Integral uniformity of 3% or better and differential uniformity □5% are routinely obtained for modern gamma camera. For radionuclide's other than ^{99m}Tc used clinically on a particular gamma camera (i.e., ^{201Tl}, ^{123}I, ^{111}In, ^{67}Ga, or ^{131}I), intrinsic uniformity should be checked at least quarterly. Spatial resolution and spatial linearity, in practice, are generally assessed semi quantitatively using some sort of resolution phantom (or mask) such as the 4-quadrant bar phantom. Such a semi quantitative (i.e., visual) assessment is faster and more convenient than actual measurement of spatial resolution of the FWHM of the line-spread function.

A 4-quadrant bar phantom consists of 4 sectors of radio opaque lead bars and intervening radio-lucent plastic strips 2, 2.5, 3, and 4 mm in width. A point source of ^{99m}Tc is placed 5 crystal dimensions from and centered over the uncollimated detector, with the phantom placed directly over the detector. A 5- to 10-million-count transmission image is then acquired and visually inspected. The lead bars in at least the 2 coarsest quadrants (i.e., with the 3- and 4-mm-wide bars) should be visually resolvable. Nowadays, at least a portion of the lead bars in the third coarsest quadrant (i.e., with the 2.5-mm-wide bars) should be visible as well. All bars should appear straight. Spatial resolution and spatial linearity should be checked with such a phantom at least weekly.

Zeinali et al. (2007) introduced and tested a newly developed computer controlled device called Adaptive Quality Control Phantom (AQCP) that designed to perform the Quality Control lest of the gamma camera. AQCP is an electro mechanic device that designed to perform a uniform set of procedure that can be used for routine quality control of a gamma camera by moving a radioactive source with the Field of View (FOV) of the camera (uniformity, COR, and CHA). The cylindrical coordinates is chosen for the motion and simulation of AQCP, combination of ball screw and reel system are used to position the point source in any desired point in space with a precision of 0.06mm, two motor was used with

accuracy of 10% (0.18 degree/step). The Haematocrit-capillaries with external diameter of 1.5 – 1.6mm and ^{99m}Tc with high specific activity (□50mCi/cc) were used to make line and point source. The AQCP was operated and controlled using specific software. SMV double head gamma camera model DSX-XL SPECT was used. System uniformity was assessed using 10mCi ^{99m}Tc-Flood source placed on the parallel hole LEHR collimator and system uniformity with AQCP was measured using line source (1mCi activity, 20% window, 10cm distance to collimator source) moved over FOV, the technologist dose was measured using electronic personal dose meter model Dose GUARD. The mean (+/- S.D) of integral Uniformity I.U parameter using IAEA-TECDOC-602 method is 9.56 (+/-0.959) while for AQCP is 9.55 (+/- 0.92) and the absorbed dose of technologist is 6.18 (+/- 0.19) µSv for IAEA method and 0.82 (+/- 0.10) µSv for AQCP method. Collimator Hole Angulations (CHA) was measured with AQCP using point source (≤ 1.6 mm diameter, 200µci of ^{99m}Tc, 20% E.W) for three collimator types LEHR, LEHS and LEUHR with 256 X 256 matrix and two image was taken for any collimator at vertical distance of 10cm and 13cm, the point source was imaged for a total of 50K counts. The approximate X and Y coordinate of each point source image is determined by calculation of the centroid of each point source image. The maximum of CHA for LEHR, LEHS and LEUHR collimator were 0.78º, 0.67º and 0.66º respectively. Center of

Rotation (COR) was calculated as IAEA-TECDOC-602 using 200µci ^{99m}Tc point source, 64 X 64 matrix , 20% energy window, each projection requires 50K count for 360^{o}. also COR was measured as AQCP by holding the camera position and AQCP moves the point source on the circle. The offset error was measured which was 0.28 deviation of X offset and 0.31 deviation of Y offset for IAEA method and 0.94 and 0.293 for X and Y offset respectively for AQCP method. The advantages of AQCP in comparison with classic methods are: reduction of radioactive material consumption, reduction of radiation exposure to the staff, reduction of QC test cost, implementation of QC program with one phantom, perform a uniform set of procedures, increase the accuracy and precision of some QC tests, automation of the measurements and evaluation process make by AQCP suitable for both acceptance tests and routine quality control checks.

Chapter Three

Methodology

3-1 Material

Nucline Spirit DH-V machine was used in this study.The average energy ofNucline Spirit was230V/50HZ and weight2,100 (4,620) kgThickness,9.5 (3/8) mm (in) (detector characteristics)with power needed 230 VAC, 15 A; 110 VAC, 30 A. The machine is hole body scan, DIMENSIONS (HXWXD), CM (IN) (detection process, HR) 165 x 145 x 120 (65 x 57 x 47), The Collimators is LEGP, LEHR, LEUHR, MEGP, HEGP data input at camera station Intel Pentium 4, 3.06 GHzThe machine is made in Hungary The advantage of this device isextra-large FOV rectangular full digital high resolution detector, highly integrated, one-board detector electronic, scanning dual-line infrared auto body contour for all collimatorseasily movable patient table made of low attenuation (< 5%) 2.5 mm thin aluminumintelligent gantry electronics with 180 and 90 or 101 degree head positionsscanning dual-line infrared auto body contour for all collimators.

3-2 Design of the study

This is an analytical case control study of SPECT Gamma Camera performance using Image Processing; where an algorithm had been developed for objective assessment.

3-3- Population and sample of the study

This study were carried out on images of quality control test in in Royal Care International Hospital; which include uniformity (integral and differential)linearity and spatial resolution, in the period from 2014 to 2016.

3-4 Method of data collection

The data of this study collected using images taken for quality control phantom, for uniformity flood phantom was used, linear Parallel equal line phantom and for resolution quadratic bar phantom:

3-4-1 Uniformity

Figure 3-1 an image show a flood phantom covered the face of gamma camera where the phantom filled with ^{99m}Tc.

The phantom flood the detector surface with uniform radiation fluxes and the counts collected by the gamma camera counting system must be uniform throughout the entire surface of the detector. This uniformity were checked using integral and differential uniformity. In the integral uniformity the developed algorithm search the image for the maximum and minim counts in the upper field of view (UFOV) and the central filed of view (CFOV) the calculate uniformity for each segment using the

following equation: *integral uniformity = ((max-count – min-counts)/ (max-count+ min-counts)) ×100*. For differential uniformity same calculation had been performed; but instead of looking for global maximum and minimum this process carried for each 5 pixel in the raw up to the end of the row then the program move to the next row and repeat the same process till the end of the rows. Then again same procedure followed in the columns for each 5 pixels in each column up to the end of the column. For uniformity same equation applied for the maximum counts and minimum in the rows as well as for columns.

Uniformity algorithm layout

```
mx=0.0
mn=0.0
im = READ_BMP('D:\\Uniformty\im1.bmp')
si=size(im)
width=si[1]
height=si[2]
factor = 1
si=size(im)
width=si[1]
height=si[2]
im2 = congrid(im, width/factor, height/factor)
window,0,xsiz=width/factor, ysiz=height/factor
tvscl, im2
```

```
;stop
window,1
;shade_surf,(im2)
ISURFACE,(im2)
;;********** Integral uniformity (IU)
mx = float(max(im2))
mn = float(min(im2))
IU = ((mx-mn)/(mx+mn))*100.
Print,'IU = ',IU,'%'
print,mx,mn******Differential uniformity
s=0
wid=si(1)/5.
DU = intarr(wid,wid)
DU(*,*)=0
im3=intarr(5)
im3(*)=0
for i = 0,wid-1 do begin
for j = 0,wid-1 do begin
im3= im[j+s:j+s+4,i:i]
s=s+4
mx = float(max(im3))
mn = float(min(im3))
U = ((mx-mn)/(mx+mn))*100.
DU(j,i)=U
endfor
```

```
s=0
endfor
print,'DU = ',max(DU),'%'
print,mx,mn
s=0
wid=si(1)/5.
DU = intarr(wid,wid)
DU(*,*)=0
im3=intarr(5)
im3(*)=0
for j = 0,wid-1 do begin
for i = 0,wid-1 do begin
 im3= im[j:j,i+s:i+s+4]
s=s+4
mx = float(max(im3))
mn = float(min(im3))
U = ((mx-mn)/(mx+mn))*100.
DU(i,j)=U
endfor
s=0
endfor
print,'DU = ',max(DU),'%'
print,mx,mn, end
```

3- 4-2-1 Linearity

System linearity depends on the camera ability to properly identify the geometric coordinates of the interaction point for a given event. The geometric distortions can be determined by imaging the slit aperture in the same way as it was done for the intrinsic spatial resolution determination followed NEMA specifications for the determination of the differential linearity and the absolute linearity. The differential linearity is defined as the standard deviation between the measured coordinates and those of the best fit to a straight line through these measured positions.The differential linearity must be specified as the mean value for the X and Y directions and for the UFOV and the CFOV.

linearity algorithm layout

```
device, decomposed=1
 READ_JPEG,'D:\Enas\dataa\Linearity\lines.jpg', im, /GRAYSCALE
im=BYTSCL(im)
im=median(im,5)
;im=hist_equal(im)
si=size(im)
width=si[1]
hight=si[2]
factor=1
im2 = congrid(im, width/factor, hight/factor)
window,0,xsiz=width/factor, ysiz=hight/factor
tvscl,im2
for i = 1, num do begin
CURSOR, X1, Y1, /device, /DOWN,/data
CURSOR, X2, Y2, /device, /DOWN,/data
y2=y1
line=im2[X1:X2, Y1:Y1]    ; vertical
window,i,xsiz=width/factor, ysiz=hight/factor
line=smooth(line,5)
window,2
plot, line
N = N_ELEMENTS(line)
```

```
X=findgen(N)

Y = line

yfit = GAUSSFIT(x, y, m1,   CHISQ=u, NTERMS=nterms)

OPLOT, x, yfit, THICK=3 ;color=4

FWHM =(round((2*SQRT(2*ALOG(2))*m1(2))))*m1(2)

line1 = FFT(line)

Amplitude = abs(line1[0:n/2+1])

print,'height',m1(0),'centre',m1(1),'width SD',m1(2),'FWHM/',FWHM/2.

print,m1(0), m1(1), m1(2), FWHM, FWHM/2

WDELETE, i

wset,0

endfor

N = N_ELEMENTS(line)

for i = 0, n-1 do begin

print, line(i)

endfor

end
```

3-4-3 Resolution

The performance of a scintillation camera system must be assessed each day of use to assure the acquisition of diagnostically reliable images.Performance can be affected by changes or failure of individual system components or subsystems and environmental conditions such as electrical power supply fluctuations, physical shock, temperature changes, humidity, dirt, and background radiation.

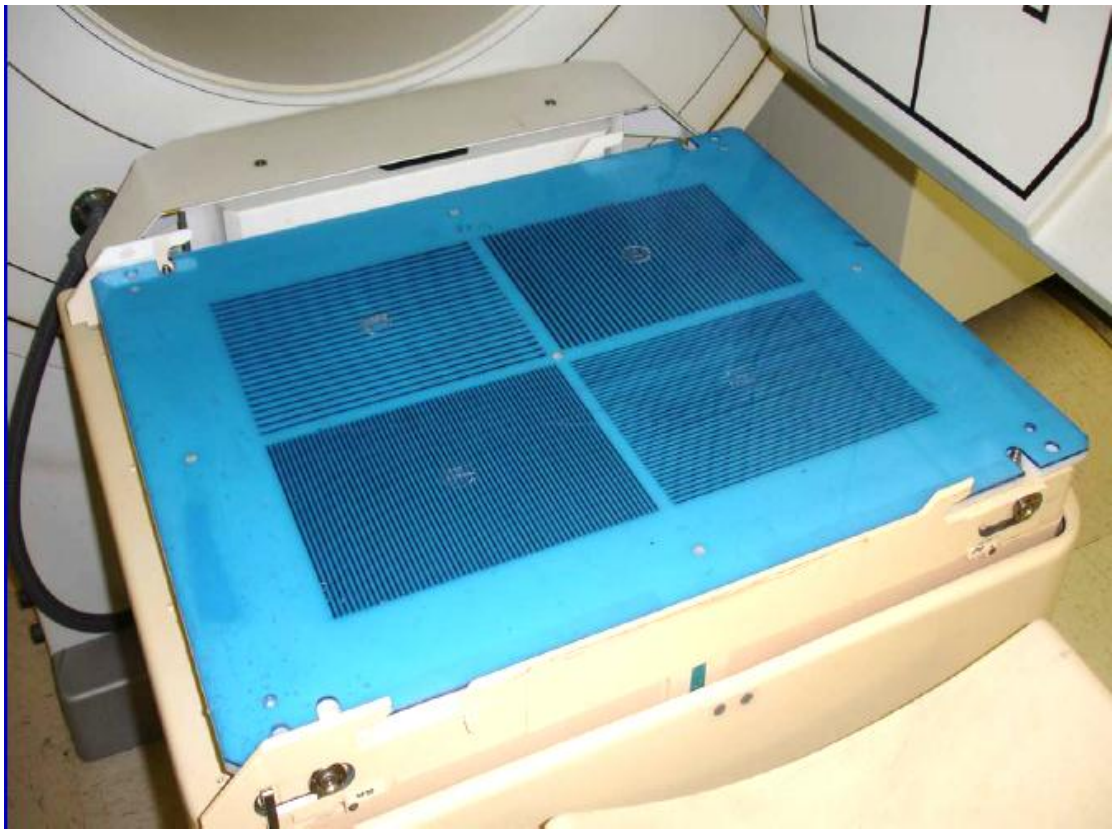

Figure 3-2 gamma camera with a quadratic bar phantom placed on top of the gamma camera detector

Figure 3-3 gamma camera with a quadratic bar phantom placed on top of the gamma camera detector and radioactive source on top of the quadratic phantom for transmission images.

Resolution recently defined as the degree of smearing of an object image and traditionally it measured as the size of the FWHM of the image for line transfer function (LTF) in pixel then this pixels were converted to mm by multiplying the number of pixel by the size of one pixel in mm, then divide the original by the measured value and multiply by 100. This

methods introduces some errors due to Dot Per Inch (DPI) approximation which depend on the image mapping process. Application of Modulation Transfer Function (MTF) will solve this problem, where the LTFs were transformed into frequency domain, then absolute value were taken to remove the negative frequencies (mirror) and then divide the frequency domain values by the maximum value and multiply by 100 to get MTF in percentage were depicted in the y-axis then in the x-axis the values of the real image bars values converted into frequency using the following equation $f = 1/2Д$ where Д is the size of the object in mm. Resolution frequency in cycle/mm will in nuclear medicine (gamma camera) will correspond to 10% MTF, then the cycle can be converted to mm to find the resolution as in the method of FWHM as shown in the algorithm below.

Resolution algorithm layout

```
device, decomposed=1;, RETAIN = 2
LOADCT, 1
READ_JPEG, 'D:\\Resolution \line image.jpg', im, /GRAYSCALE
;tota=0.
im=ROTATE(im, 1)
si=size(im)
width=si[1]
hight=si[2]
factor = 2
```

```
im2 = congrid(im, width/factor, hight/factor)

window,0 ,xsiz=width/factor, ysiz=hight/factor

tvscl, im2

LTF_line1=im[100:250,300:300]

LTF_line1=smooth(LTF_line1,13)

window,2

plot, LTF_line1

N = N_ELEMENTS(LTF_line1)

X=findgen(N)

Y = LTF_line1

yfit = GAUSSFIT(x, y, m1, NTERMS=nterms)

OPLOT, x, yfit, THICK=3 ;color=4

FWHM =round(10/(2*SQRT(2*ALOG(2))*m1(2)))

print,'wire thickness= 10  ','height = ',m1(0),'  Centre =',m1(1), '       Width (SD)
=',m1(2),'    FWHM = ',FWHM

line1 = FFT(LTF_line1)

Amplitude = abs(line1[0:n/2-1])

MTF=(Amplitude(0)/m1(0))*100.

print, Amplitude(0), ' MTF =  ',MTF

t=histogram(amplitude)

s=N_ELEMENTS(t)

print,(s/m1(0))*100

window,1

plot, LTF_line1

nn=n_elements(LTF_line1)
```

```
for i = 0,nn-1 do begin
print,LTF_line1(i)
endfor
end
```

Chapter four

Results

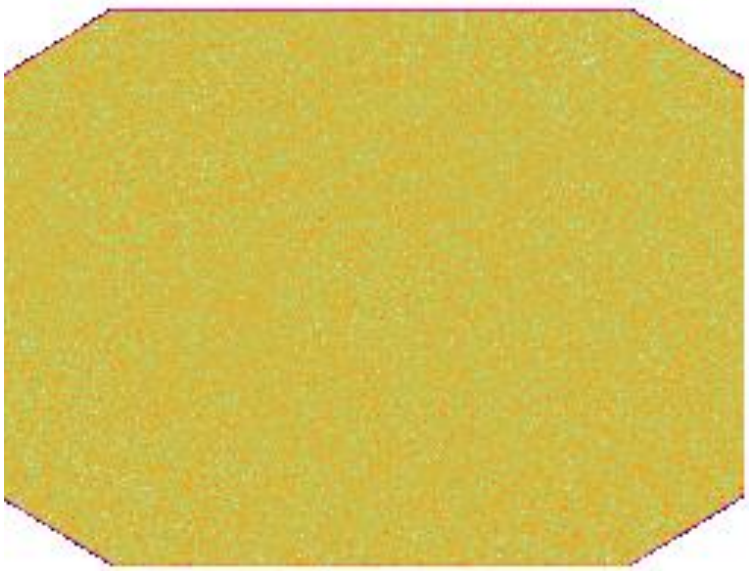

Figure 4-1 Routine intrinsic uniformity image, ^{99m}Tc, and 20% energy window set symmetrically over the 140 keV photopeak of 99mTc. For integral uniformity the Minimum counts 7132, maximum counts 7554 and for differential max counts 7132 and minimum counts 7554

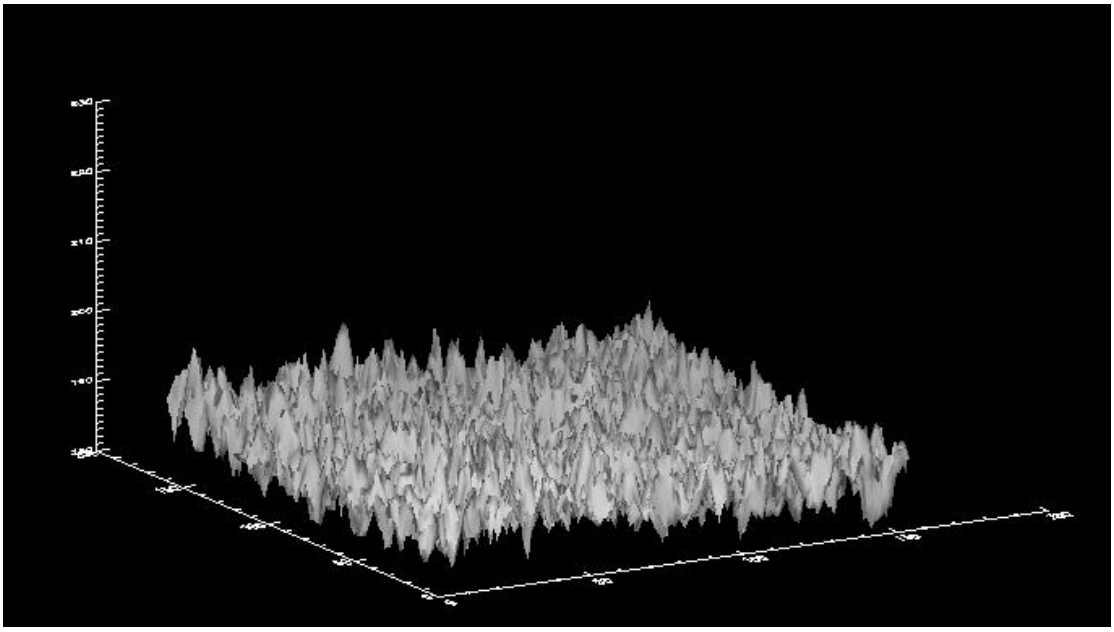

Figure 4-2 shade surface plot of the uniformity image shows non-uniform image subjectively.

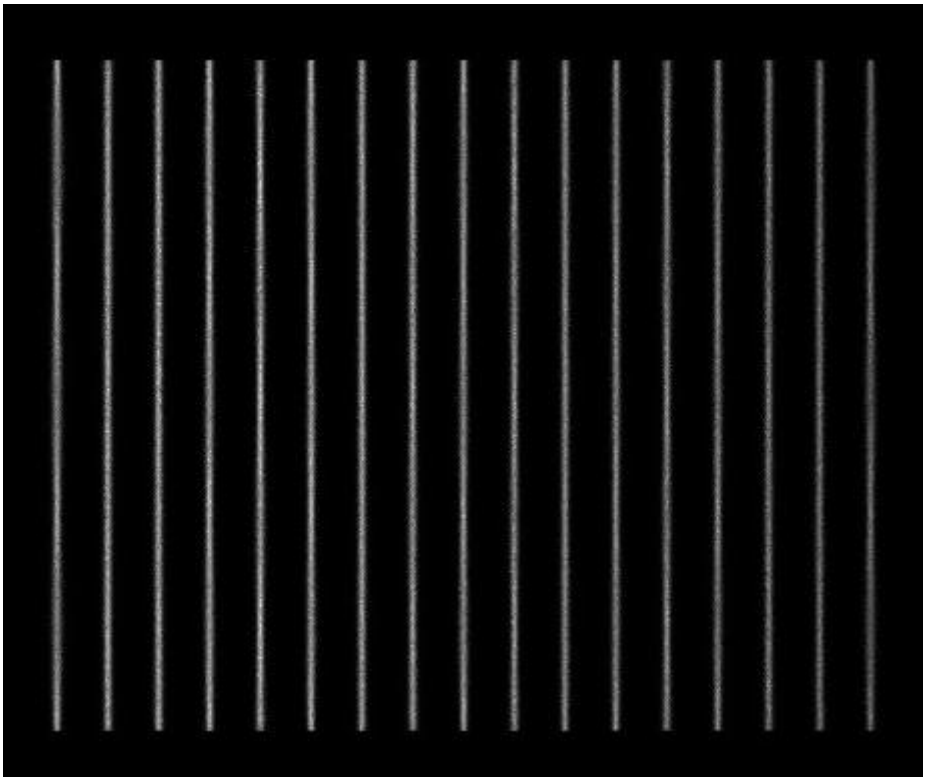

Figure 4-3 gamma camera image of Parallel-line equal-space (PLES) phantom with slit equal to one mm and a distance between them equal 30 mm arranged in X-direction.

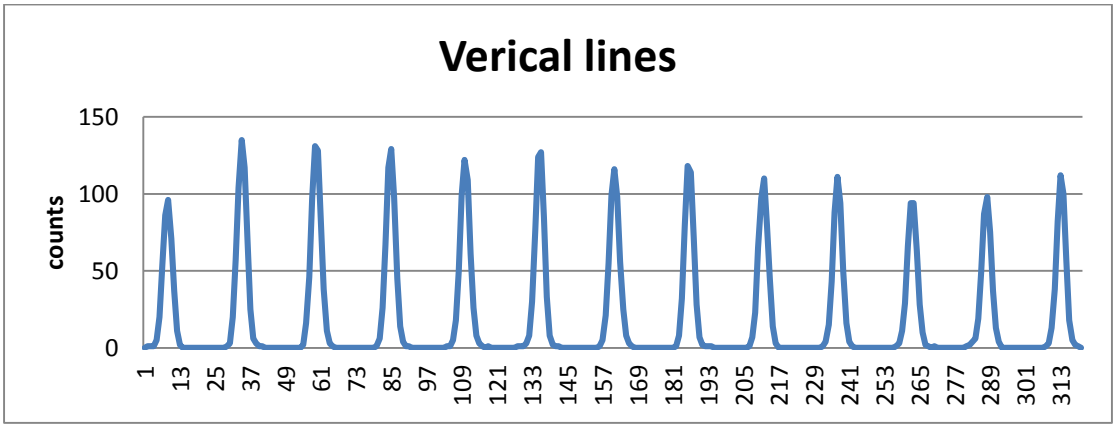

Figure 4-4 line graphs of the counts across the PLES phantom in the vertical position for the center field of view.

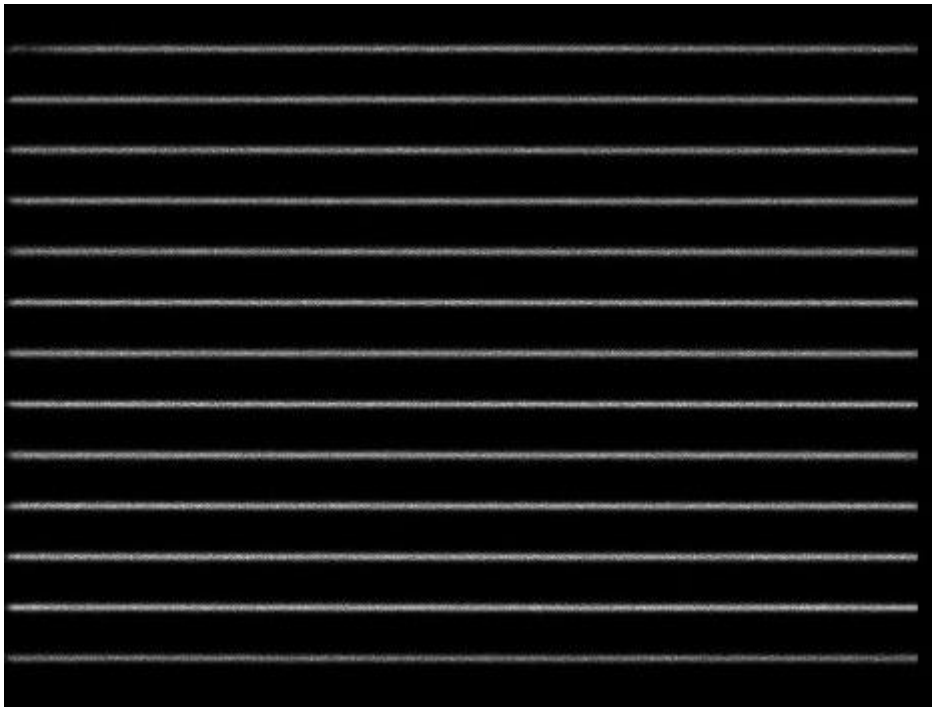

Figure 4-5 gamma camera image of Parallel-line equal-space (PLES) phantom with slit equal to one mm and a distance between them equal 30 mm arranged in Y-direction

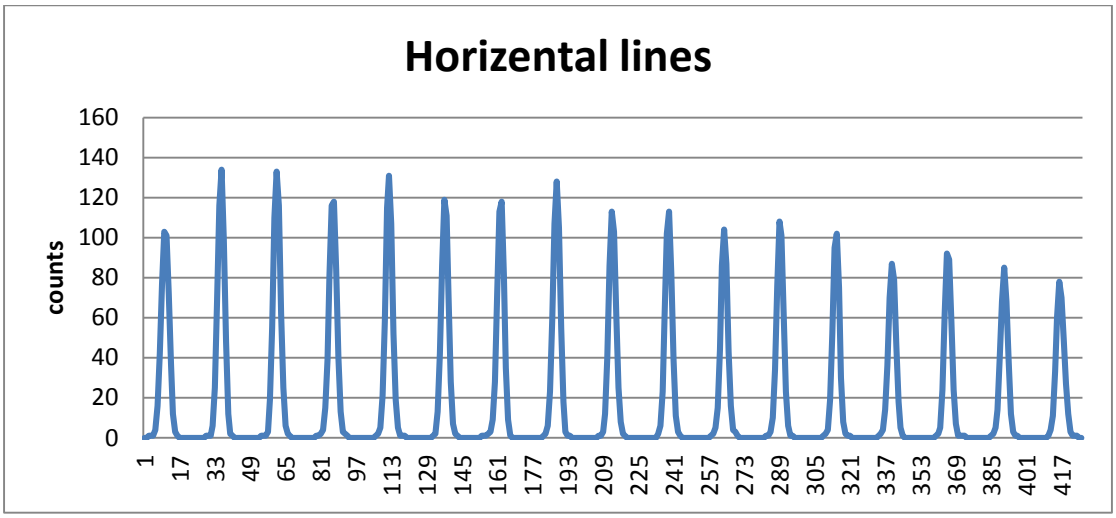

Figure 4-6 line graphs of the counts across the PLES phantom in the horizontal position for the center field of view.

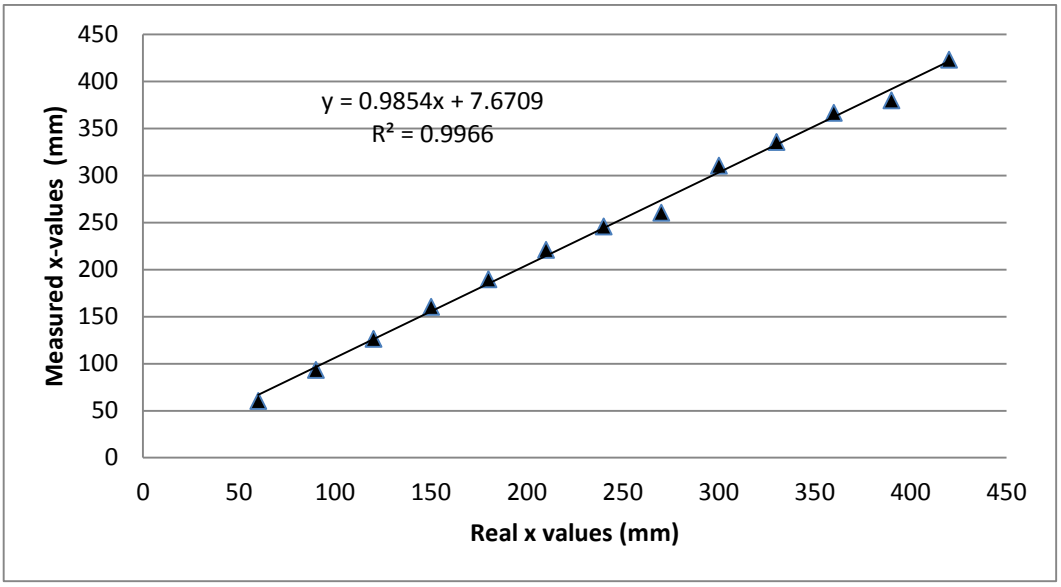

Figure 4-7 scatter plot show a direct linear relationship between the real locations of the slits in the phantom and the central peaks of the counts in the vertical image that corresponds to the real location by fitting a curve on the line spread function graph

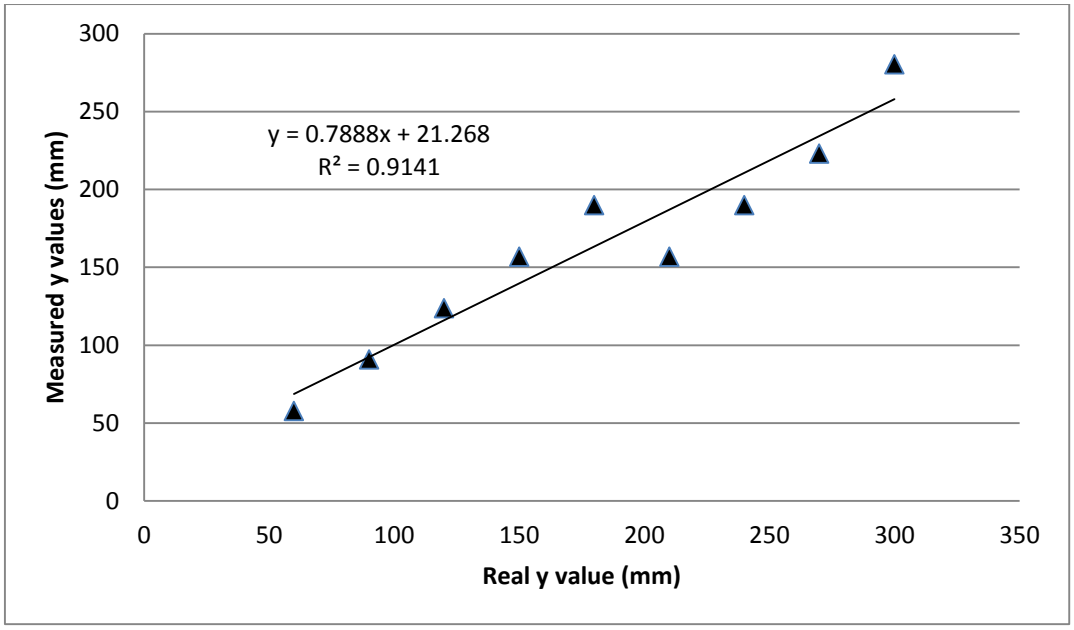

Figure 4-8 scatter plot show a direct linear relationship between the real locations of the slits in the phantom and the central peaks of the counts in the horizontal image that corresponds to the real location by fitting a curve on the line spread function graph

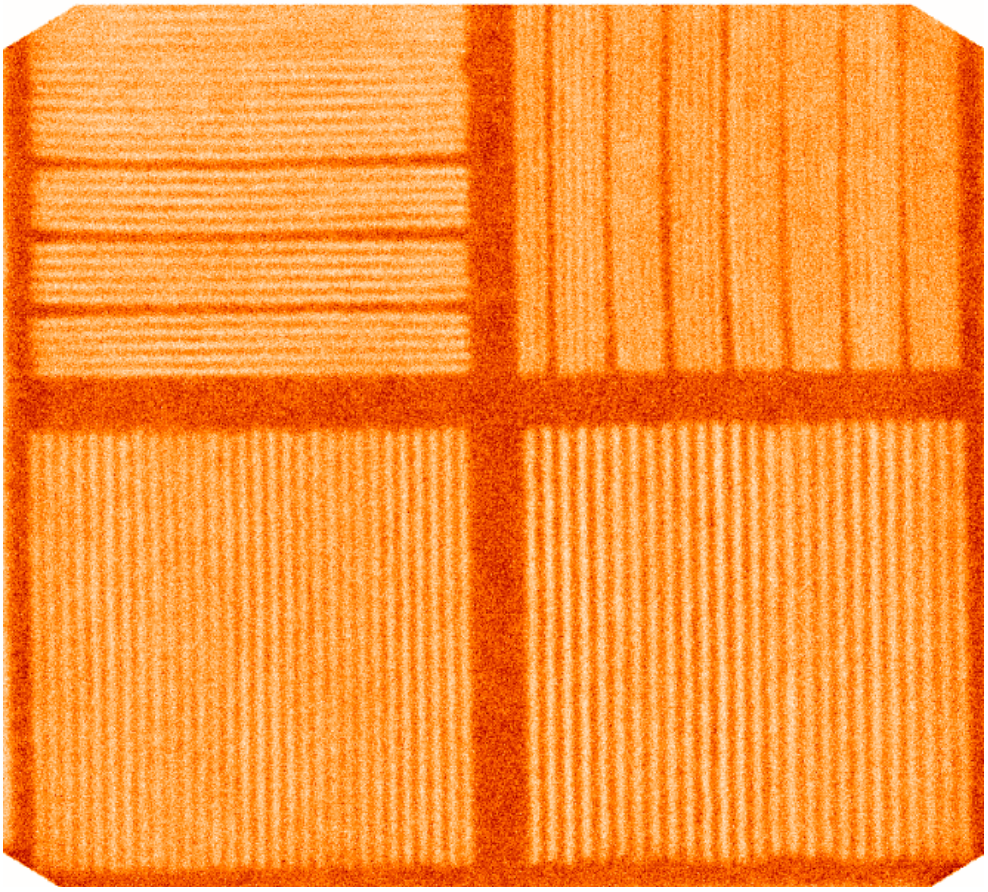

Figure 4-9 gamma camera image for a quadratic bar phantom with different slits size to measure the resolution

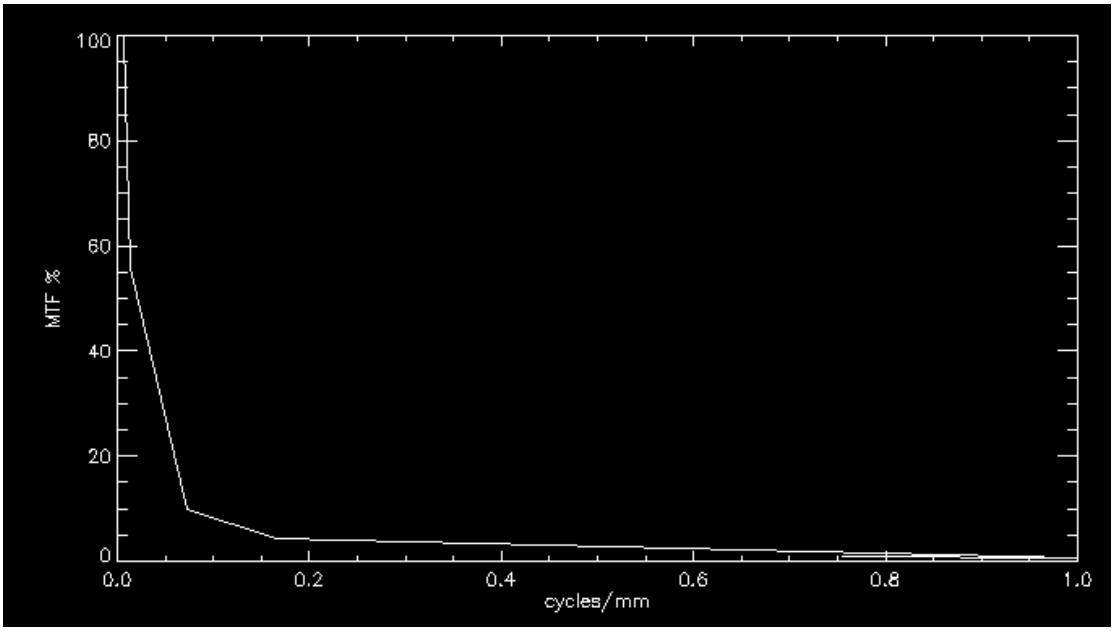

Figure 4-10 a line graph show modulation transfer function of the different thickness of the quadratic phantom versus frequencies of the slits size to find the resolution frequency of gamma camera at 10% MTF.

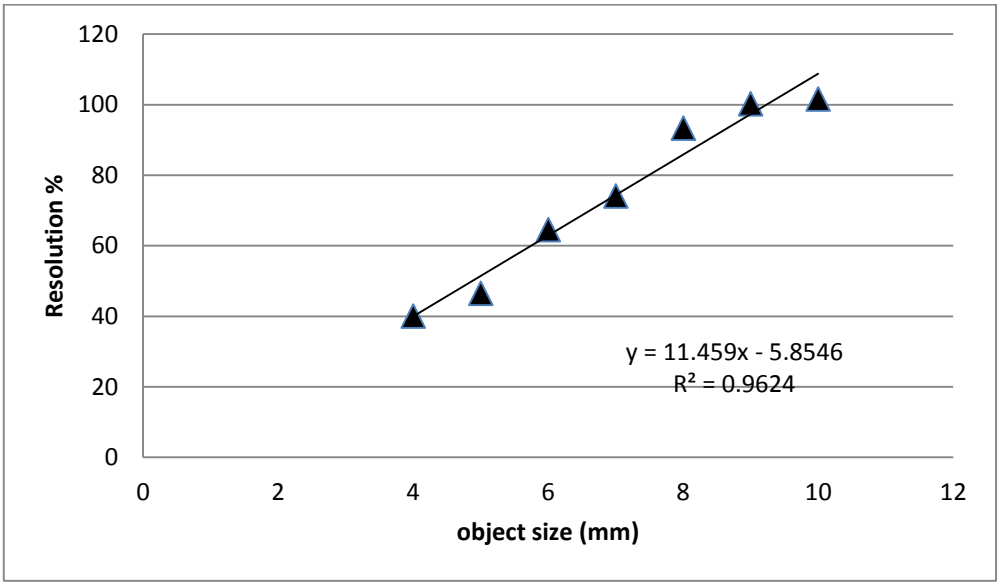

Figure 4-11 scatter plot of the object size (size of the slit) versus resolution, it shows a direct linear relationship.

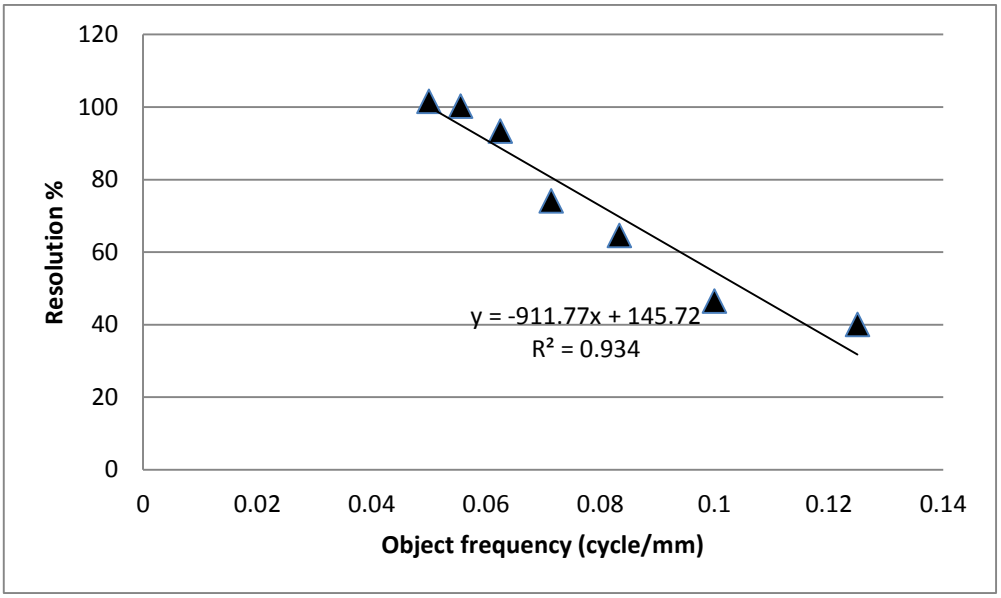

Figure 4-12 scatter plot of the object frequency (frequency of the slit size) versus resolution, it shows a indirect linear relationship.

Chapter five

Discussion, Conclusion and Recommendation

5-1 Discussion

The most basic measure of gamma camera performance is flood-field uniformity. This is the ability of the camera to depict a uniform distribution of activity as uniform. It is assessed by "flooding" the camera with a uniform field of radiation and then assessing the uniformity of the resulting image. The integral and differential uniformity for UFOV and CFOV was measured for image in Figure 4-1 using an algorithm generated by the researcher where it search for the maximum and minimum counts for booth model of uniformity; UFOV integral uniformity was 2.87% and differential uniformity raw and column was 1.69% and 1.53% respectively. For CFOV integral uniformity was 2.97%. While row differential uniformity was 1.96% and column differential uniformity was 1.55%. The results of uniformity showed that the level of uniformity was within the tolerance range i.e. <5%; but usually correction map were generated for perfection. Uniformity instead of mathematical representation which is an objective method; it can be perceived using shade-surface plot where uniformity can be easily depicted and te region of problem can be identified as shown in

Figure 4-2.

Linearity the amount of positional distortion or displacement of the measured position of photons relative to the actual position where those detected photons entered the detector i.e. for the geometrical linearity, the LSF are fitted and the standard deviation is compared to a line. In this study the researcher adopt a new method to find the rate of change in position using a linear relationship between the actual location and the measured one; where the actual being the independent one (plotted in the x-axis). As shown in Figure 4-7 and 4-8 where the points generated from Figure 4-5 and 4-6 for the vertical and horizontal image (Figure 4-3 and 4-4) by fitting curve one the line spread function to find the peak which equal to the location of the FWHM/2 as intensity on the x-axis. The linear scatter plot for vertical (Figure 4-7) indicates that the measured value increased by 0.98 mm per 1 mm of the actual location of the line; the differences was 0.02 mm which indicates that almost the points falls in the line with a correlation coefficient of 0.998. Therefore variation between the actual and measured line location was within a good tolerance, concerning the vertical positions. For horizontal the linear relationship between the actual and measured showed that the measured increased by 0.8mm/1mm; i.e. the difference between the two in average equal to 0.2mm, with a correlation coefficient equal to 0.956; which

indicate a good tolerance but relatively low than the vertical line. This difference mainly attributed to statistical variation rather than uniformity problem which affect linearity at the end.

The spatial resolution of the Gamma camera increases with an object size (mm) increases (Figure 4-11). The resolution for minimum object used 4mm was 70% and increased with object size increased to reach 100% resolution for an object size of 10 mm i.e. Resolution = 11.45%/mm of object size.

Resolution also could be measured using MTF making benefit of frequency domain properties; where the resolution of gamma camera usually correspond to frequency that match 10% of MTF value in gamma camera images. In this study as shown in graph 4-12 there is indirect linear relationship between the frequency of the object and resolution; which means the resolution decreases as the object frequency increases because the increases of frequency means decreases of object size and vice versa, the linear scatter plot reveals that the resolution % decrease by 911.7%/cycle /mm; also the graphs showed that the resolution which correspond to the coordinate of the MTF at 10% and frequency of 0.05cycle /mm

The result of RICK camera represent 10% resolution at object frequency 0.05 and 0.06 while the result of RICH camera showed 10% resolution at object size of 0.05 gives 100%

5-2 conclusion

This study as it aim to quantify the quality control of SPECT gamma camera images using developed algorithm it make it possible to objectively to have quantitative analysis of a crucial type of test concerning SPECT gamma camera.

There is several algorithms in addition to the visual inspections method to assess gamma camera but both method either it depend on the manufacturer who developed the algorithm, so it is abdicable for only one device or in case of visual perception it depends on the experience and the visual characteristics of the observer.

The developed algorithm can be used objectively and improved as required without looking for expertise from other country, as well it can be made to check the acceptance of the device performance regardless the built in programs.

5-3 Recommendations

- Application of the developed algorithm to assess other gamma camera devices with comparison with the built in routine.
- Incorporation of the other SPECT gamma camera QC test parameters in the developed algorithm.
- Developed of indigenous phantom that can suit the developed algorithm as well as the QC standard, because the available one used for visual and electronic quantification.
- A development of a routine that can be used to assess SPECT QC test images rather than planner one.

Reference:

Zanzonico. P 2008 Routine Quality Control of Clinical Nuclear Medicine Instrumentation: A Brief Review , J Nucl Med.,7th edition , p1-7

Fred A. M and Milton J. G, 2012. Essentials of Nuclear Medicine Imaging, Journal name, 6th edition , p55-60

Gopal .B, Saha 2013 Physics and Radiobiology of Nuclear Medicine Springer Science & Business Media, 2nd edition
P 164-166

A Vickery, T Jørgensenand R de Nijs 2011 NEMA NU-1 2007 based and independent quality control software for gamma cameras and SPECT Journal of Physics 317 (2011) 012023 p1-4

A.H.Ng, K.H.Ng, Dharmendra H., Perkins A.C. 2009 A low-cost phantom for simple routine testing of single photon emission computed tomography (SPECT) cameras , Applied Radiation and Isotopes 67
p 1864–1867

Seret.A 2001 NEMA NU1-2001 performance tests of four Philips Brightview cameras, journal of science direct Elsevier p 589-591

Rova .A, Celler.A , and Hamarneh .G 2008, Journal of Digital Imaging, Vol 21, No 2, 2008: p 243-254

Michael K. O'Connor, Mayo Clinic, Rochester, 2000 Quality Control of Scintillation Cameras (Planar and SPECT) p1-9

Minarik .D, Gleisner .K and jungberg .M L 2008 Evaluation of quantitative 90Y SPECT based on experimental phantom studies, physics in medicine and biology vol 53 p 5690-5702

Porras. E, Escat. B, Benlloch J.M. D. Hanifi.K, Lopez .S, Pavon. N. Ruiz .J.A., Sanchez .F, Sebastia. A 2002 Portable mini gamma camera for medical applications , J. Elsevier Science p 186-189

Elshemey.E , Ghoneim.A, Khader.H 2013 Scattered radiation effects on the extrinsic sensitivity and counting efficiency of a gamma camera ,J. Elsevier Science p18-21

Ferreira. F, Souza .D 2011 Liver phantom for quality control and training in nuclear medicine , J Elsevier Science p791-792

Beekman.F and Gerralt .A 2005 Photon-counting versus an integrating CCD-based gamma camera : important consequences for spatial resolution , J physics in medicine and biology 50 P109-118

Jeon .H, Cho .G 2008 The detective quantum efficiency (DQE) for evaluating the performance of a small gamma camera
system with a uniformly redundant array (URA) collimator J Elsevier Science p279-281

Jeon .H, Kim.H , Cha.B, YulKim.J , Cho.G, Chung.H, Yun.H 2009 Performance evaluation for pinhole collimators of small gamma camera by MTF and NNPS analysis: Monte Carlo simulation study J Elsevier ,p 93-95

Islamian.J, Toossi.M, zhad.M, Naseri.S, l Ljungberg .M 2012 Simulation of a Quality Control Jaszczak Phantom with SIMIND Monte Carlo and Adding the Phantom as an Accessory to the Program Iranian Journal of Medical Physics, Vol. 9, No. 2, p135-138

StadenJ.A, RaanH.U, Lotter.M.G, Aswegen .A.V and Herbst c.p 2007 Production of radioactive quality assurance phantoms using a standard inkjet printer ,Phys. Med. Biol. **52** ,p 329-336

Lees.J.E , Bassford.D.J , Blake.O.E , Blackshawb.P.E and. Perkins.A.C 2011 A high resolution Small Field Of View (SFOV) gamma camera: a columnar scintillator coated CCD imager for medical applications J IOP science 6 C12033, p1-10

Ejeh .J, Adedapo.K ,Bidemi.A, Akinlade.I , Osifo.O 2011 Gamma camera intrinsic uniformity in an unstable power supply environment , Technical Note, Hellenic Journal of Nuclear Medicine, P 1-3

Ueno.K, Hattori.K , Ida.C , Iwaki.S, Kabuki.S,
Kubo.H, Kurosawa.S, Miuchi.K , Nagayoshi.T , Nishimura.H, Orito.R, Takada.A
, Tanimori . T 2008 Performance of the gamma-ray camera based on GSO(Ce) scintillator array and PSPMT with the ASIC readout system J Elsevier Science, Nuclear Instruments and Methods in Physics Research A 591 p269-271

Koike.T; Uno.S , Uchida.T , Sekimoto.M . Murakami.T . Shoji.M , Nagashima.F , Yamamoto.K and Nakano.E 2012 A new gamma camera with a Gas Electron Multiplier , J IOPscience 7 C01078, p1-9

Lees.J.E , Bassford.D.J , Blackshaw.P.E .Perkins .A.C2010 Design and use of mini-phantoms for high resolution planar gamma cameras Applied Radiation and Isotopes 68, science direct J Elsevier , p2448-2450

Holstensson.M , Partridge.M, Buckley.S and Flux.G

2010 The effect of energy and source location on gamma camera intrinsic and extrinsic spatial resolution: an experimental and Monte Carlo study , Phys. Med. Biol. 55 , p1735-1749

Perez.C , Leonel. A. Aroche.T, Bejerano.G , Mayor.R , Corona.C , and Lopez.A 2008; Establishment of a National Program for Quality Control of Nuclear Medicine Instrumentation , J Nucl Med Technol, p203-205

Jeong.M , Choi.Y , Chung.Y , Song.T , Jung.J , Hong.K , Min.B , Kyung.Y , Lee.H and Kim.B 2004 Performance improvement of small gamma camera using NaI(Tl) plate and position sensitive photo-multiplier tubes , Phys. Med. Biol. 49,p 4961-4968

Holen.R , Stefaan .V and enberghe, Staelens.S and Lemahieu. I 2008 Comparing planar image quality of rotating slat and parallel hole collimation: influence of system modeling , Phys. Med. Biol. 53,p1989-2001

BAECHLER.S , Corminboeuf.S , linder , Trueb.P.H , malterre.J , bischof.d , elaloye.F, bochud.F,verdun.R 2008 Feasibility of the gamma camera acceptance testing producer introduced by the Swiss federal office of public health , NU-1, 2001 ,p1-6

Yamamoto.S , Imaizumi.M , segawa.E , HatazawaJ 2010 Development of a compact and high spatial resolution gamma camera system using LaBr (Ce) J Elsevier,p 261-266

Sokole.E & Płachcínska .A& Britten.A 2010 Routine quality control recommendations for nuclear medicine instrumentation, Eur J Nucl Med Mol Imaging 37:662–671 , p 662-669

Starck.S , Båth.A , and Carlsson.S 2005 The use of detective quantum efficiency (DQE) in evaluating the performance of gamma camera systems, Phys. Med. Biol. 50 , p 1601-1608

Fidler.V , Prepadnik.M and Xie .Y 2001 Upgrading of gamma cameras for developing countries , Radiol Oncol ,35(1) ,p1-8

Zeinali.H , Nejad.M and Mirzaii .A 2007 Design an Adaptive Quality Control Phantom to Optimize QC Test Methods The Open Medical Imaging Journal, p 1-5